Heliyon 10 (2024) e35157

Contents lists available at ScienceDirect

Heliyon

journal homepage: www.cell.com/heliyon

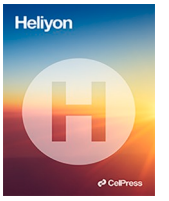

Research article

Machine learning-driven mast cell gene signatures for prognostic and therapeutic prediction in prostate cancer

Abudukeyoumu Maimaitiyiming [a,b,1], Hengqing An [a,b,c,**,1], Chen Xing [a,b,c], Xiaodong Li [a,b,c], Zhao Li [d], Junbo Bai [e], Cheng Luo [a,b], Tao Zhuo [a,b], Xin Huang [a,b], Aierpati Maimaiti [a,f], Abudushalamu Aikemu [g], Yujie Wang [a,b,c,*]

[a] The First Affiliated Hospital, Xinjiang Medical University, Urumqi, China
[b] Department of Urological, Urology Centre, The First Affiliated Hospital of Xinjiang Medical University, Urumqi, Xinjiang, China
[c] Xinjiang Clinical Research Center of Urogenital Diseases, Urumqi, China
[d] Department of Abdominal Ultrasonography, The First Affiliated Hospital of Xinjiang Medical University, Urumqi, Xinjiang, China
[e] Department of Pediatric Urology, Urology Centre, The First Affiliated Hospital of Xinjiang Medical University, Urumqi, Xinjiang, China
[f] Department of Neurosurgery, Neurosurgery Centre, The First Affiliated Hospital of Xinjiang Medical University, Urumqi, Xinjiang, China
[g] Department of Emergency Medicine, Youai Hospital, Urumqi, Xinjiang, China

ARTICLE INFO

Keywords:
Prostate cancer
Mast cell markers
Transcriptomics analysis
Computational biology
Patient stratification
Predictive biomarker

ABSTRACT

Background: The role of Mast cells has not been thoroughly explored in the context of prostate cancer's (PCA) unpredictable prognosis and mixed immunotherapy outcomes. Our research aims to employs a comprehensive computational methodology to evaluate Mast cell marker gene signatures (MCMGS) derived from a global cohort of 1091 PCA patients. This approach is designed to identify a robust biomarker to assist in prognosis and predicting responses to immunotherapy.

Methods: This study initially identified mast cell-associated biomarkers from prostate adenocarcinoma (PRAD) patients across six international cohorts. We employed a variety of machine learning techniques, including Random Forest, Support Vector Machine (SVM), Lasso regression, and the Cox Proportional Hazards Model, to develop an effective MCMGS from candidate genes. Subsequently, an immunological assessment of MCMGS was conducted to provide new insights into the evaluation of immunotherapy responses and prognostic assessments. Additionally, we utilized Gene Set Enrichment Analysis (GSEA) and pathway analysis to explore the biological pathways and mechanisms associated with MCMGS.

Results: MCMGS incorporated 13 marker genes and was successful in segregating patients into distinct high- and low-risk categories. Prognostic efficacy was confirmed by survival analysis

Abbreviations: PCA, Prostate Cancer; TCGA, The Cancer Genome Atlas; LASSO, The least absolute shrinkage and selection operator; MCMGS, Mast cell marker gene signature; BCR, Biochemical recurrence; CRPC, Castration-resistant prostate cancer; PSA, Prostate-specific antigen; AUC, Area under the curve; GEO, Gene Expression Omnibus; GO, Gene Ontology; KEGG, Kyoto Encyclopedia of Genes and Genomes; RSF, random survival forests; GBM, Generalized boosted regression modeling; GSEA, Gene Set Enrichment Analysis; TME, Tumor microenvironment; PFS, progression-free survival; TMB, tumor mutation burden.

* Corresponding author. Department of Urology, Urology Centre, The First Affiliated Hospital of Xinjiang Medical University, Urumqi, Xinjiang, China.

** Corresponding author. An Department of Urology, Urology Centre, The First Affiliated Hospital of Xinjiang Medical University, Urumqi, Xinjiang, China.

E-mail addresses: 9269735@qq.com (H. An), wangyjmn@163.com (Y. Wang).

[1] These authors have contributed equally to this work.

https://doi.org/10.1016/j.heliyon.2024.e35157
Received 1 February 2024; Received in revised form 23 July 2024; Accepted 24 July 2024
Available online 26 July 2024

incorporating MCMGS scores, alongside clinical parameters such as age, T stage, and Gleason scores. High MCMGS scores were correlated with upregulated pathways in fatty acid metabolism and β-alanine metabolism, while low scores correlated with DNA repair mechanisms, homologous recombination, and cell cycle progression. Patients classified as low-risk displayed increased sensitivity to drugs, indicating the utility of MCMGS in forecasting responses to immune checkpoint inhibitors.

Conclusion: The combination of MCMGS with a robust machine learning methodology demonstrates considerable promise in guiding personalized risk stratification and informing therapeutic decisions for patients with PCA.

1. Introduction

Prostate cancer has become one of the most common malignant tumors affecting men's health worldwide and is also one of the main causes of high mortality from male cancers [1]. Data from GLOBOCAN 2022 shows that there are approximately 1.46 million new cases of prostate cancer diagnosed, and more than 390,000 deaths occur due to this disease, ranking sixth among male cancer mortality cases [2]. Recurrence is a common occurrence in nearly half of localized PCA patients, despite undergoing curative treatments like radical prostatectomy (RP) or radiation therapy [3]. The same holds for chemotherapy [4] and hormone therapy [5]. As a consequence, a large proportion of individuals diagnosed with localized PCA will eventually develop castration-resistant prostate cancer (CRPC). Among them, patients experiencing biochemical recurrence (BCR) exhibit clinical manifestations characterized by tumor relapse and metastasis, ultimately leading to an incurable state and death [6]. Existing indicators, including Gleason score and prostate-specific antigen (PSA), have limitations in accurately predicting the time of biochemical recurrence (BCR) in PCA patients. The substantial heterogeneity of PCA undermines the predictive capability of conventional markers, leaving prognostic biomarkers largely unexplored. Consequently, there is an imperative to investigate novel biomarkers that can enhance predictive models and unveil new prognostic and treatment efficacy indicators.

The tumor microenvironment (TME) is an intricate system consisting of immunological cells, stromal cells, extracellular matrix molecules, and cytokines that interact with tumor cells [7]. There is mounting evidence that the TME's constituent parts are essential to the development and spread of tumors. In addition to affecting a patient's prognosis, dysregulated TME alterations may also be used as immunotherapy biomarkers [8]. The involvement of non-immune cells has received less attention, despite the present emphasis on anti-tumor immunity, with a focus on adaptive T-cell responses. Nonetheless, PCA treatment with immunotherapy has lately gained popularity [9]. FDA-approved immunotherapies for PCA include Sipuleucel-T (a dendritic cell-based therapy) and pembrolizumab (PD-1/PD-L1 axis-targeting checkpoint inhibitor), with other approaches currently being investigated in clinical trials [10]. Mast cells (MCs) have long been recognized for their central role in allergic reactions. However, their involvement in tumor development and the tumor microenvironment has become increasingly apparent, where they not only promote tumor growth and angiogenesis but also aid in the evasion of immune system attacks by tumor cells [11-13]. In various types of cancer, the density of mast cells is significantly elevated, contributing to tumor growth and metastasis. For instance, in renal cell carcinoma (KIRC), the presence of mast cells correlates with a poor prognosis [14]. In breast cancer, mast cells aid in prognostic prediction for patients with lung metastasis from breast cancer, yet their function and prognostic significance remain contentious, as they may exert both tumor-promoting and anti-tumor effects [15,16]. In glioblastoma, mast cells play a pivotal role in tumor angiogenesis and reshaping the tumor microenvironment (TME), and they can serve as a potentially effective prognostic factor for glioblastoma [17]. The relationship between mast cells and PCA has only recently begun to gain recognition in the scientific community [18-21]. Intratumoral mast cells may act as prognostic biomarkers following prostatectomy [22]. However, no studies have yet reported the biological functions of MCs in the onset of prostate cancer. Given the complex role of mast cells in the tumor microenvironment and their diverse actions across different cancer types, an in-depth investigation into the function of mast cells in prostate cancer is imperative. This will not only enhance our understanding of the tumor immune microenvironment but may also uncover novel therapeutic strategies to improve the prognosis and treatment outcomes for patients with prostate cancer.

The use of single-cell RNA sequencing (ScRNA-seq) has led to a dramatic improvement in our ability to characterize the molecular features of TME immune cell populations. Researchers have previously used scRNA-seq to determine the molecular characteristics of TME immune cells, which has led to the construction of gene signature models that may predict prognosis and immunotherapy efficacy in cancer patients [23,24]. However, there is limited research employing scRNA-seq data to explore the molecular analysis, prognosis, and treatment disparities of Mast cells within the TME of prostate cancer (PRAD) patients, necessitating further investigation.

In this study, we comprehensively analyzed PRAD using scRNA-seq data to uncover the molecular characteristics of infiltrating Mast cells and determine the specific marker genes. Subsequently, we developed a Mast cell marker gene signature (MCMGS) using a machine-learning approach and predicted prognostic features in PRAD using TCGA RNA-seq data. The GEO-independent cohort was used to validate MCMGS's predictive ability. Additionally, we investigated the associations between MCMGS and factors such as tumor immune microenvironment, genomic heterogeneity, treatment response, and drug selection for PCA. Our findings offer potential biomarkers and therapeutic strategies with significant clinical implications for managing PCA.

2. Materials and methods

2.1. Data collection and processing

Multiple databases were utilized in this study to obtain data for analysis. ScRNA-seq datasets (GSM5793828, GSM5793829, GSM5793831, GSM5793832) related to PCA based on GSE193337 were retrieved from GEO (www.ncbi.nlm.nih.gov/geo) to identify Mast cell marker genes in prostate adenocarcinoma (PRAD). In addition, the overall tumor transcriptome data of 501 PRAD patients, along with their clinical information, were retrieved from UCSC Xena (https://xenabrowser.net/) using TCGA. Samples with fewer than 30 days of follow-up or those without relevant clinical data were not included, resulting in 494 patients' clinical data used for constructing the training set, identifying survival-related genes, and developing prognostic features. Clinical and RNA-seq data from additional datasets, including GSE70770, GSE46602, ICGC (PRAD-CA and PRAD-FR), DKFZ, and E-MTAB-6128, encompassing a total of 597 patient samples, were obtained from various sources such as the International Cancer Genome Consortium (ICGC), cBioPortal, and ArrayExpress (Fig. 1).

Transcriptome data underwent quantile normalization, background correction, and log2 transformation. The results presented as fragments per kilobase of transcript per million mapped reads (FPKM) were translated to the values for transcripts per kilobase of transcript per million (TPM). For genes with duplicates or multiple probes corresponding to a single gene, the average expression value was utilized. Genes with an average expression value below 1 were excluded from the analysis. The data that were used in this investigation were obtained from several internet databases that are open to the general public and had already obtained ethical approval from the original studies.

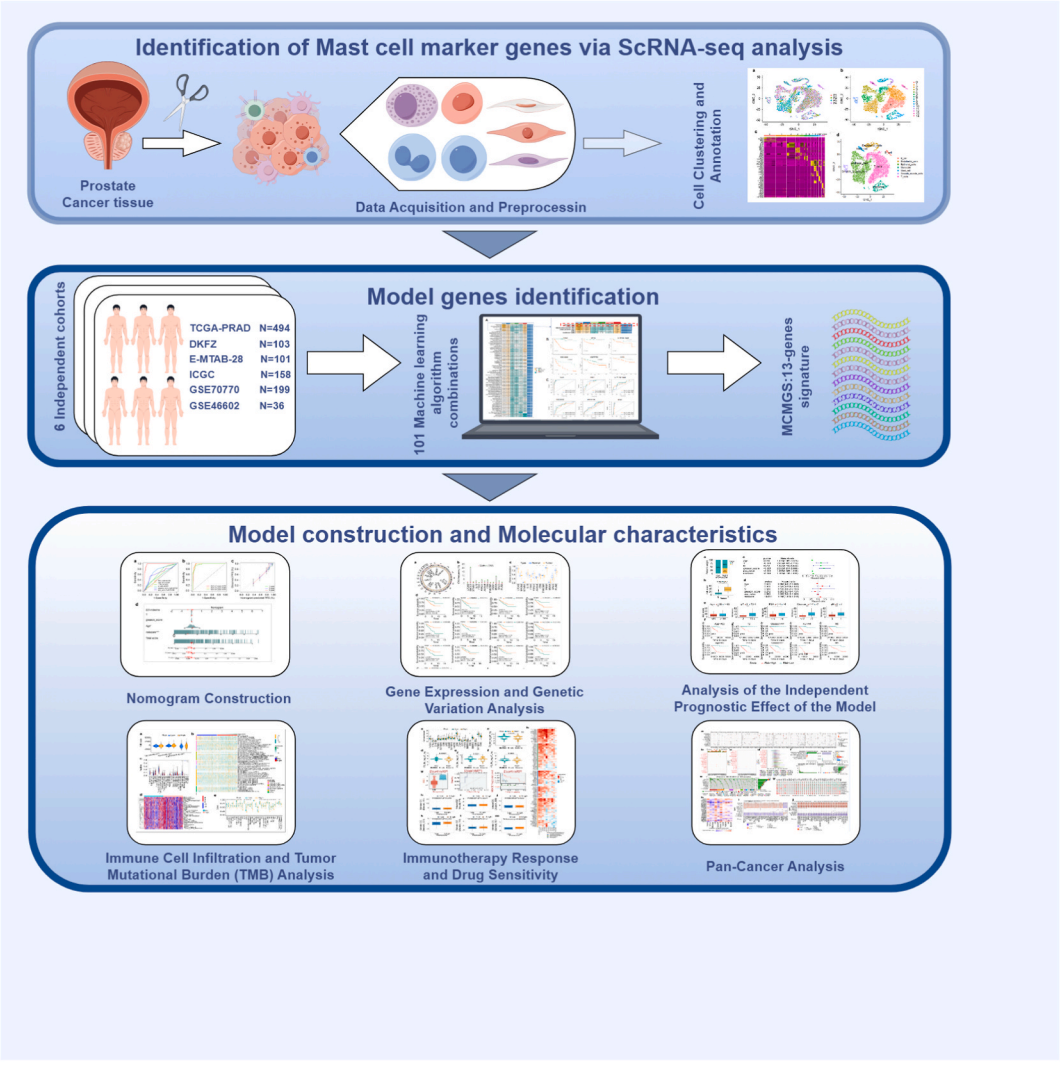

Fig. 1. Flowchart.

2.2. Identification of Mast cell marker genes via ScRNA-seq analysis

To identify the genes associated with Mast cells, a ScRNA-seq study was conducted. We utilized the harmony [25] algorithm for data integration, processing multiple distinct scRNA-seq datasets obtained from the GEO database for PCA. Based on the top 15 corrected Harmony embeddings and the FindNeighbors function, cells were clustered downstream. Annotation of cell types was performed using the singleR package after visualizing cell clusters with the t-SNE function. We annotated the clusters based on reference data from the human primary cell atlas [26]. We conducted a differential gene expression analysis utilizing the Wilcoxon-Mann-Whitney test through FindAllMarkers to detect the differentially expressed genes (DEGs) within each cell subpopulation. Adjusted p-value <0.01 and $|\log2 \text{(fold change)}| > 1$ were used as threshold parameters to identify genes that serve as markers for Mast cells.

2.3. Mast cells-based prognostic model construction by machine learning

Gene expression profiles of Mast cell markers in PCA were retrieved from the TCGA database. We conducted univariate Cox regression analysis to identify marker genes for Mast cells. We combined 10 different machine learning methods to produce a stable and accurate consensus model; survival support vector machine (survival-svm), generalized boosted regression modeling (GBM), supervised principal components (SuperPC), Cox partial least squares regression (plsRcox), Cox boost, stepwise Cox, Ridge, Lasso, elastic net (Enet), and random survival forests (RSF).

To fit predictive models for prognostically relevant Mast cell marker genes, 101 algorithm combinations were evaluated on the TCGA-PRAD cohort. Furthermore, each model was tested on five validation datasets (GSE70770, GSE46602, ICGC cohort, DKFZ, and E-MTAB-6128). We determined which model had the greatest average Harrell's concordance index (C-index) across all validation datasets. Prognostically relevant Mast cell marker genes (MCMGS) in prostate cancer were identified for further investigation.

Marker genes for prostate adenocarcinoma (PRAD) advancement were evaluated via univariate Cox regression analysis in the training set, with progression-free survival (PFS) as the primary clinical endpoint. Prognostic genes were identified depending on their statistical significance, utilizing a p-value threshold of <0.01. PFS was chosen as the primary clinical endpoint due to its established reliability in the context of prostate cancer [27]. Specifically, PFS is measured as the time duration between the diagnosis date and the occurrence of new events, encompassing cancer progression, local recurrence, distant metastasis, or death resulting from cancer.

2.4. Validated risk characterization of the MCMGS model

Patients were classified into high-risk and low-risk groups (categories) based on an optimal model as per the median risk score of MCMGS. The survival ROC tool was employed to compute the area under the curve (AUC) for the feature genes in the training and testing datasets, especially for 1-, 3-, and 5-year prediction intervals, to evaluate the prognostic potential of MCMGS. To assess statistical significance, we used Kaplan-Meier (KM) analysis and log-rank test with the aid of the "survminer" R package. The predictability of the features was evaluated through survival analysis across five independent datasets and AUC validation.

2.5. Comparison of MCMGS with other published markers

We conducted a retrospective review of previously published articles on genes associated with prostate cancer prognosis. From these studies, we collected the genes included in the constructed models. The gene expression data were proportionally normalized and multiplied by their respective coefficients to obtain a score for each sample. Then, we calculated the area under the curve (AUC) for each signature to compare its predictive ability. We compared the MCMGS with other publicly available signatures.

2.6. MCMGS as an independent prognostic indicator for PRAD

Clinical data from various datasets, including TCGA, DKFZ, E-MTAB-392, GSE70770, GSE46602, and ICGC, were utilized in this study. The dataset consisted of patients who had their entire follow-ups recorded, as well as their survival status, providing information on variables like T stage, N stage, age, Gleason score, and PSA levels. After including all of these clinical factors using univariate and multivariate Cox regression analyses, a further analysis was carried out to ascertain whether the risk score generated by MCMGS maintained its significance. Furthermore, a Kaplan-Meier (KM) survival analysis was employed to examine the prognostic significance of MCMGS in various clinical subsamples of PCA patients included in the PFS prediction model. This analysis compared the variations in survival rates between high-and low-risk patients in each clinical group.

2.7. Developing a nomogram for use in predictive analysis

The "survival" and "rms" R packages were used in the development of the nomogram, incorporating age, T stage, Gleason score, and risk score. The nomogram was used to provide a visual representation of the predicted survival outcome for PRAD patients. Additionally, to determine how well the nomogram-predicted results matched up with actual outcomes, a calibration curve was drawn. The chosen feature genes' accuracy in predicting patients' survival outcomes was verified using C-index curves. These analyses aimed to provide a robust predictive model for PRAD patient survival and examine how well each factor contributes to a prognosis.

2.8. Functional enrichment analysis

With the aid of the "clusterProfiler" R package, we conducted Gene Ontology (GO) and KEGG (Kyoto Encyclopedia of Genes and Genomes) pathway analyses. ClusterProfiler's enriched GO functions were used for GO analysis, while the org.Hs.eg.db database from the Bioconductor project was used to annotate the genome. The most up-to-date version of the KEGG database was retrieved via a web API, and the "enrichKEGG" function was used for the KEGG analysis. Significantly enriched pathways were identified using a p-value threshold of <0.05.

2.9. Gene set enrichment analysis (GSEA)

The prognostic gene signature's molecular mechanisms were investigated by GSEA utilizing Java GSEA software. Biological process (BP) pathways associated with high-risk patients were identified by querying the annotated gene set c5.go.bp.v7.2.symbols.gmt. Statistical significance was determined by setting the threshold at FDR <0.05 and $|NES| > 1$, indicating the enrichment of biologically relevant pathways.

2.10. Immune cell infiltration analysis and estimation of stromal and immune fractions

The CIBERSORT algorithm is a valuable tool for extracting immune cell infiltration profiles of 22 different types of cells from gene expression data. In this study, to compare immune cell infiltration levels between high- and low-risk categories, we used the CIBERSORT method. Additionally, to assess the extent of stromal and immune cell infiltration using gene expression data, we used the ESTIMATE method from the "ESTIMATE" R package. The TCGA PRAD cohort's RNA sequencing data were employed to determine matrix scores, immune scores, estimate scores, and tumor purity scores. Furthermore, these scores were compared across risk categories by means of Wilcoxon t-tests, enabling the examination of variations in the tumor microenvironment across diverse risk categories.

2.11. Prediction of the response to immunotherapy

To predict how well a patient will respond to immune checkpoint blockade (ICB) treatment, we included three factors: T-cell receptor (TCR) repertoire, tumor mutation burden (TMB), and PD-L1 expression. PD-L1 mRNA expression in PRAD patients was determined using TCGA RNA sequencing data. The TCGA database was searched for gene mutation information for PRAD patients, and TMB was then computed utilizing "maftools" package. TMB represented the count of somatic insertions and substitutions per million bases within coding regions of the genome. We employed the comprehensive TISIDB platform (http://cis.hku.hk/TISIDB/) to examine the link between PRAD patients' gene expression levels, immune subtypes, and therapeutic targets.

2.12. Drug sensitization and small book drug identification

Using the "pRRophetic" R package, both high-risk and low-risk patients were evaluated for treatment responses. The package determines the half-maximal inhibitory concentration (IC50) on the Genomics of Drug Sensitivity in Cancer (GDSC) dataset for each PRAD patient. The GDSC dataset, containing information on drug sensitivity genomics, is available at [28] (https://www.Cancerxgene.org/). This analysis aims to provide insights into the potential therapeutic efficacy and individualized treatment response within different risk categories of PRAD patients.

2.13. Pan-cancer analysis of MCMGS characterized genes

For each cancer type, our analysis focused on comparing the expression profiles between the tumor and adjoining non-tumor tissues. Specifically, the gene expression patterns of signature genes (log2FC > 1.5, FDR <0.05) were examined. We used TCGA to analyze clinical data from 33 tumor samples, thus determining whether there was a correlation between gene expression profiles and patient survival. Subsequently, based on mRNA values, tumor samples were categorized into low and high-expression groups, and survival time and status were fitted within these groups using the SURVIVAL R package. Each gene in each type of cancer was subjected to a log-rank test and a Cox proportional hazards model. Additionally, SNV data were collected from a total of 10,234 samples across 33 different types of cancer. We compiled a summary of the data utilizing a percentage heatmap to acquire a further understanding of the overall mutation frequency in pan-cancer. We meticulously analyzed copy number variation (CNV) data from 11,495 tumor samples within the TCGA database to detect significant genomic amplifications or deletions among the participants. This analysis aimed to uncover the genomic alterations associated with the MCMGS genes that could potentially influence cancer progression and patient outcomes. Amplifications and deletions were considered concerning homozygosity to enhance the detection of each gene alteration. High-frequency CNVs were defined as those with a frequency exceeding 5 %. Lastly, we compared the methylation levels of each gene between tumor and non-tumor samples utilizing Wilcoxon signed-rank tests and identified genes showing significant hypomethylation or hypermethylation using a probability value threshold of 0.05.

2.14. Statistical analysis

The Spearman correlation analysis was conducted to examine the relationships that existed between the variables. Hazard ratios (HR) were calculated utilizing univariate and multivariate Cox regression models, and forest plots visualized the regression coefficients. LASSO regression addressed overfitting concerns in constructing the predictive model. Wilcoxon rank-sum tests compared categorical variables across risk groups. Univariate and multivariate Cox regression analyses were conducted to investigate the predictive significance of MCMGS as well as its link to clinical-pathological characteristics. The level of statistical significance was established at $P < 0.05$. R software, v R4.2.1 (http://www.r-project.org/), was applied for both data analysis and generation. Data analysis and graphical generation were both conducted using the R software, version R4.2.1 [R Core Team (2023). R: A language and environment for statistical computing. R Foundation for Statistical Computing, Vienna, Austria. URL http://www.r-project.org/].

3. Result

3.1. Defining mast cell marker gene expression profiles in prostate cancer

To ensure high-quality scRNA-seq data, we utilized four PCA scRNA-seq datasets (GSM5793828, GSM5793829, GSM5793831, GSM5793832) from GSE193337. Genes expressed in at least three cells and cells expressing at least 200 genes were retained. Ultimately, GSM5793828 contained 2420 cells, GSM5793829 contained 5724 cells, GSM5793831 contained 5087 cells, and GSM5793832 contained 5964 cells. The Harmony method was applied to integrate the four prostate cancer samples (Fig. 2a), resulting in the identification of 14 cell clusters (Fig. 2b).Subsequently, the cell types within each cluster were annotated using the Human Primary Cell Atlas reference data [29] as well as the research data from Isabel Heidegger et al. [30] Cluster analysis also revealed unique patterns of gene expression, with known marker genes differentially expressed across various cell clusters as shown in Fig. 2c. Among them, mast cells were defined as the cells found in the 12th cluster (Fig. 2d), with 168 genes (Supplementary Table 1). GO and KEGG functional enrichment analyses demonstrated their association with immune features such as myeloid leukocyte activation, mast cell activation, T cell activation, and leukocyte activation involved in immune response (Supplementary Figs. 1a and b).

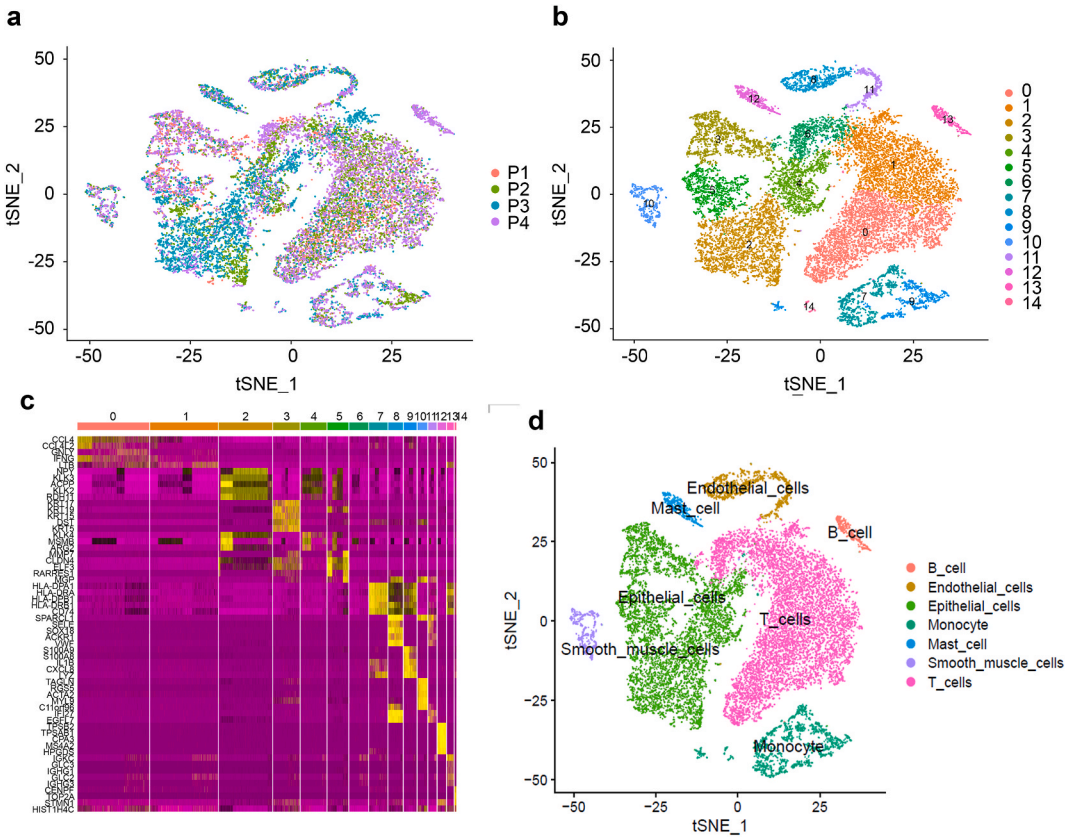

Fig. 2. Identification of Mast cell marker genes by sc-RNAseq. (a) T-SNE plot of 19,195 cells from 4 prostate cancer samples. (b) Identification of 14 cell clusters. (c) Each cell cluster's top 5 marker genes, shown in a heatmap. (d) Cell type identification using marker genes.

3.2. Characterization of mast cell marker gene construct models

Considering PFS as the disease progression time, 168 Mast cell marker genes from the TCGA-PRAD dataset were analyzed using univariate Cox regression to generate a prognostic MCMGS. We identified 35 significant prognostic Mast cell marker genes (Supplementary Table 2). In a 10-fold cross-validation framework, ten machine learning algorithms (Survival-SVM, Enet, GBM, step-wise Cox, SuperPC, Cox boost, Ridge, Lasso, plsRcox, and RSF) were applied to identify Mast cell marker genes with the highest C-index in the TCGA PRAD training and testing sets. The datasets used for analysis included DKFZ, E-MTAB-28, ICGC, GSE70770, and GSE46602 (Fig. 3a). The optimal C-index was obtained by the integration of the CoxBoost and RSF algorithms, and using this model, we identified 13 valuable genes that constitute the optimal MCMGS (FTH1, STMN1, LTC4S, TYROBP, GALC, BACE2, MSRA, ANXA4, PLIN2, CD9, IL13, P2RX1, PRNP) (Supplementary Table 3).

The median risk score obtained by sorting the MCMGS risk scores was applied to classify patients into low-and high-risk categories. Fig. 3b depicts the distribution of survival status among various risk score groups, showing that the high-risk patients had a lower survival duration relative to those at low risk across multiple datasets. The area under the ROC (AUC) values were computed for PFS at

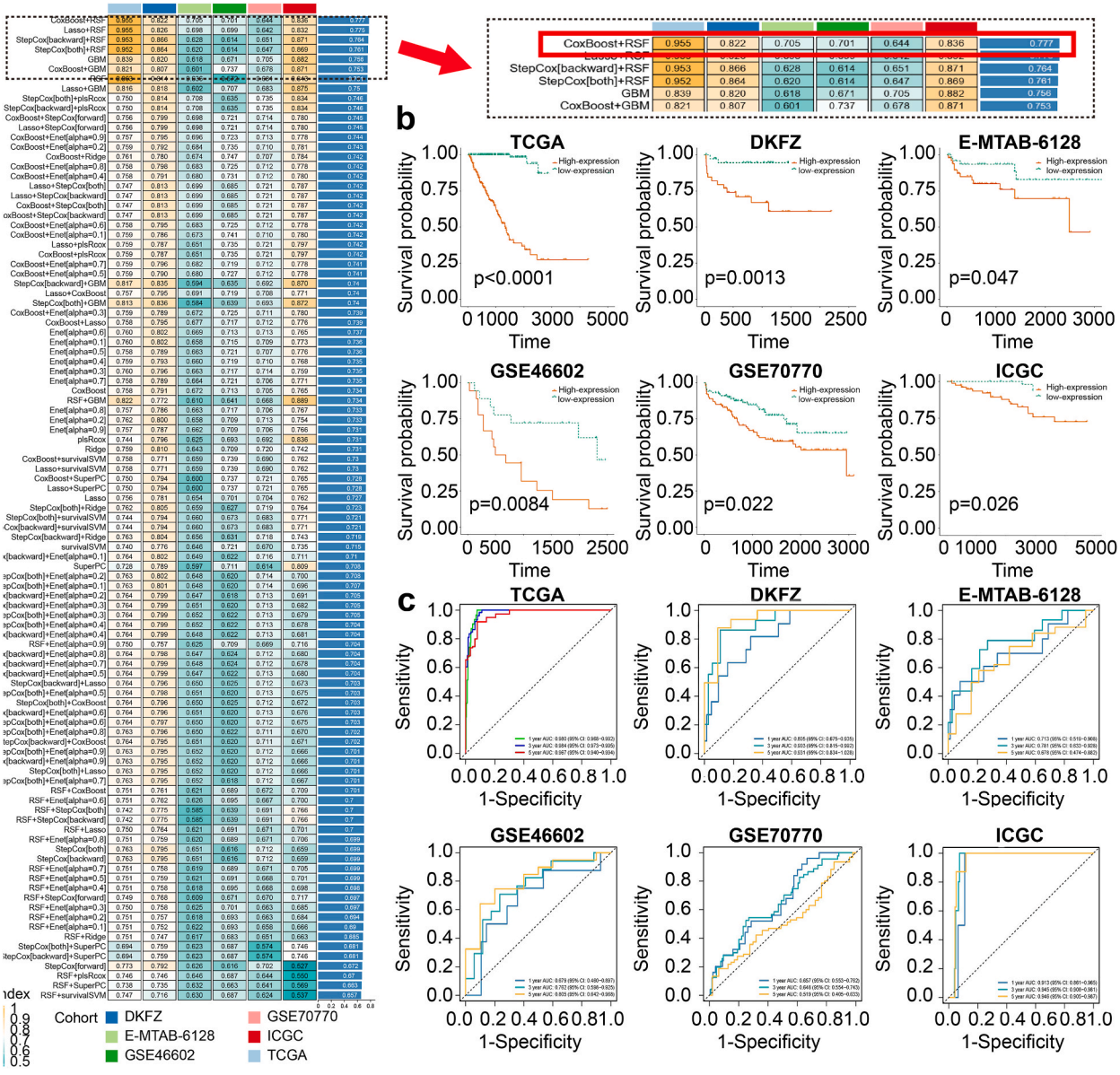

Fig. 3. Construction and validation of the MCMGS model using 101 machine learning methods. (a) C-index is computed for every model across all datasets., with the CoxBoost + RSF combination yielding the highest C-index. (b) Survival curves by MCMGS in TCGA-PRAD, DKFZ, E-MTAB-6128, GSE46602, GSE70770, and ICGC datasets. (c) Each dataset's ROC curves for 1-, 3-, and 5-year PFS.

1, 3, and 5 years in different datasets to assess the prediction accuracy of the MCMGS risk model. The AUC values were as follows: TCGA PRAD dataset (0.979, 0.985, 0.972), DKFZ dataset (0.807, 0.834, 0.878), E-MTAB-6128 dataset (0.709, 0.755, 0.661), GSE46602 dataset (0.679, 0.763, 0.823), GSE70770 dataset (0.663, 0.677, 0.602), and ICGC dataset (0.910, 0.933, 0.927). These results highlight the robust prognostic value of the MCMGS signature (Fig. 3c).

3.3. Evaluation and validation of the MCMGS model

Clinical variables such as Gleason score, serum PSA, TNM staging, age, and tumor percentage are commonly used for guiding the management and prognostication of PCA. In this study, we compared the C-index of these variables with the risk scores generated by our constructed MCMGS. Moreover, we compared MCMGS with ten previously published prostate cancer signatures and found that in the TCGA PRAD cohort, MCMGS demonstrated a higher AUC value of 0.979 when compared to other markers (Supplementary Fig. 1c, Supplementary Table 4). These results underscore the high predictive performance of our MCMGS model, enabling improved prognostication of survival outcomes in prostate cancer patients.

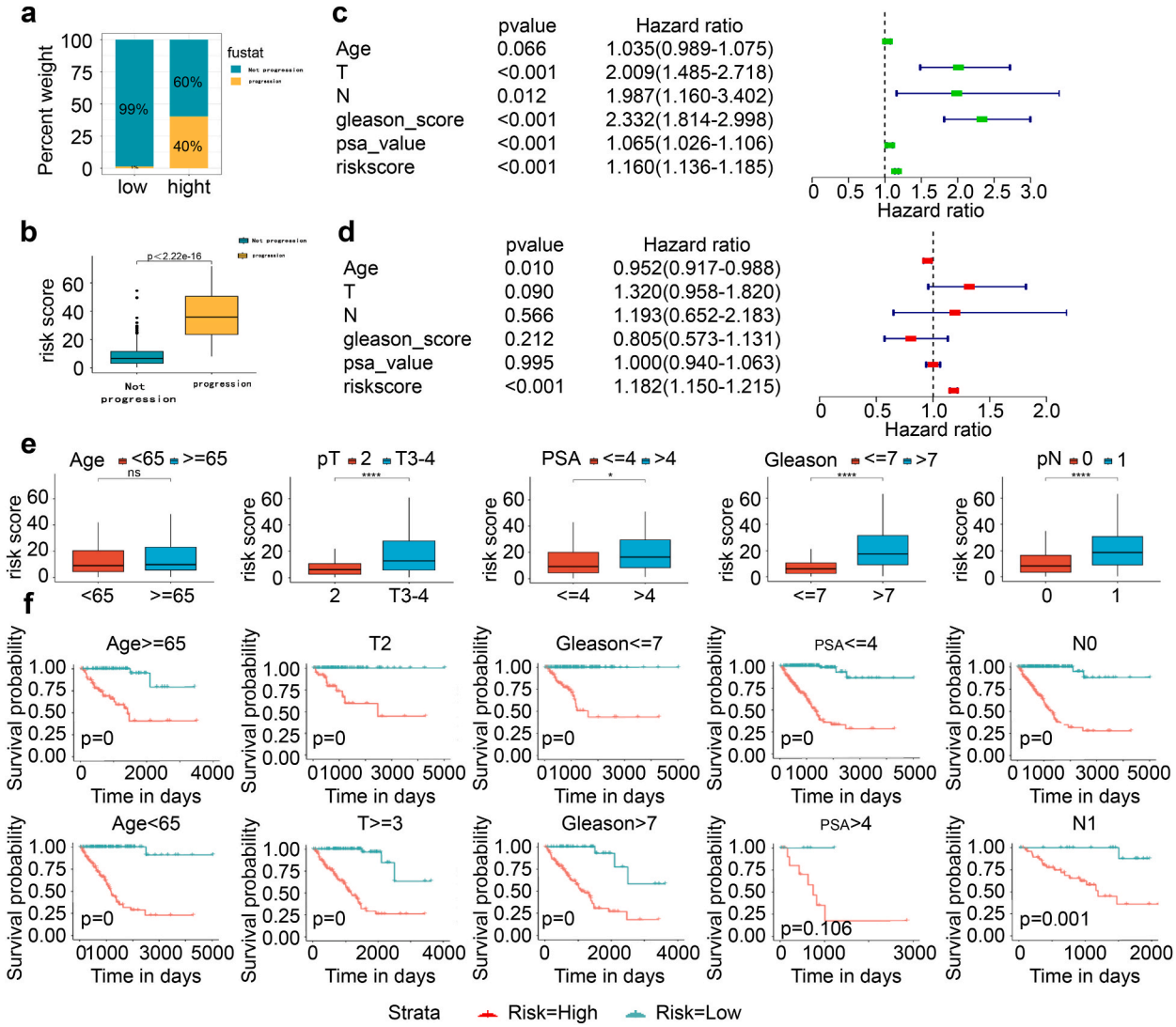

Fig. 4. Clinical subtype analysis of MCMGS: (a),(b) Proportions and variations in disease progression between high- and low-risk groups in the TCGA PRAD dataset. (d): Univariate, and (d): multivariate Cox regression analysis with various clinical characteristics. (e) Differences in high- and low-risk groups across different T-stage, PSA, Gleason score, and N-stage groups. (f) Risk scoring based on MCMGS gene features as a valuable prognostic marker for adverse outcomes in various clinical-pathological groups. MCMGS differentiates high-risk patients based on clinical-pathological features: age, Gleason score, T stage, PSA, and N stage. *$p < 0.05$; ****$p < 0.001$; ns, no statistical significance.

3.4. Independent prognostic effect of MCMGS in patients with PRAD and analysis in different clinical subtypes

In the TCGA PRAD patient cohort, a higher proportion of disease progression cases (40 %) was noted in the high-risk patients relative to only 1 % in those at low-risk. Compared to patients who did not experience disease progression, those who did had considerably higher risk scores ($p < 2.22e\text{-}16$) (Fig. 4a and b). To evaluate the independent predictive power of MCMGS in the prognosis of PCA individuals, clinical parameters and risk scores of PRAD patients from the TCGA dataset were analyzed via univariate and multivariate analyses. In the TCGA dataset, the MCMGS risk score was shown to independently function as a prognostic factor of PFS (HR: 1.182, 95 % CI: 1.150–1.215, $p < 0.001$) (Fig. 4c and d). Furthermore, within the TCGA PRAD cohort, the prognostic power of the risk score was assessed across many age groups, T-stages, N-stages, Gleason scores, and PSA levels. The analysis revealed significantly higher risk scores in patients with T3-4 stage tumors, N1 stage tumors, high PSA (PSA>4 ng/ml), and high Gleason score (Gleason>7) ($p < 0.05$, Fig. 4e). Additionally, across all clinical groups of PRAD patients, high-risk scores were strongly correlated with a worse prognosis ($p < 0.001$, Fig. 4f). Overall, these data illustrate that MCMGS independently serves as a predictive factor for risk stratification and PFS in PCA patients.

3.5. MCMGS-based risk model construction nomograms

The model's predictive accuracy for PRAD patients was assessed by ROC curve analysis. The AUC values for risk score-based predictions at 1-year, 3-year, and 5-year time points were high (Fig. 5a) (AUC = 0.979, 0.985, 0.972), demonstrating a high degree of model specificity and sensitivity. Importantly, compared to traditional clinicopathological features, the risk score (AUC = 0.979) exhibited superior prognostic capability for PRAD patients (Fig. 5b). We created a nomogram for PRAD patients that takes into account their T-stage, Gleason score, age, and risk score to improve the generated risk model's clinical value and usability (Fig. 5c). The data confirmed that the risk score had the greatest impact on predicting PFS, which indicates that the risk model based on the 13 MCMGS genes can accurately predict PRAD. The calibration plot demonstrated satisfactory consistency between predicted and observed probabilities at 1-, 3-, and 5-year PFS (Fig. 5d), further confirming its practicality in predicting patient prognosis.

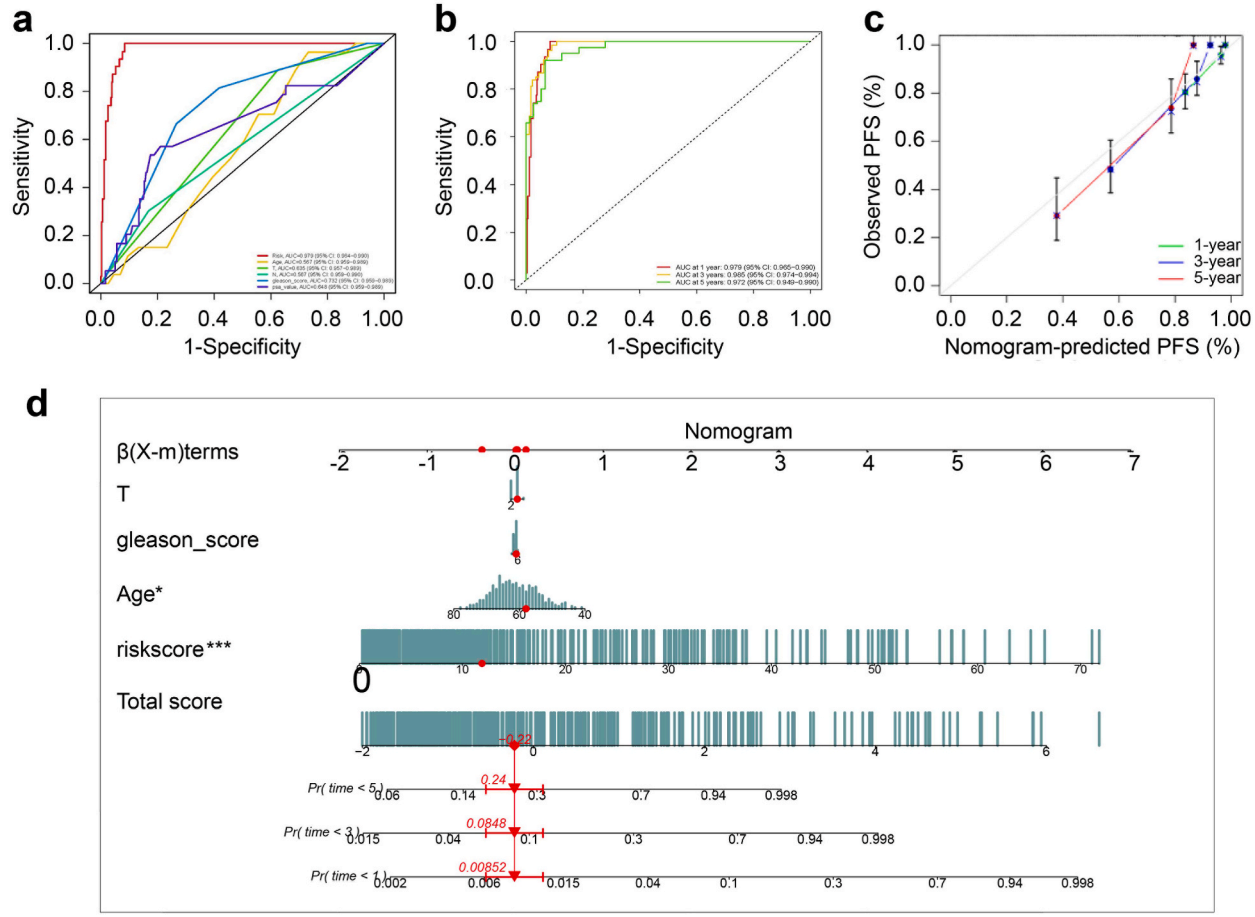

Fig. 5. Construction of column charts based on clinical features. (a) ROC curve analysis over time. (b) Multi-index ROC analysis. (c) Nomogram prediction of 1, 3, and 5-year PFS in PRAD patients. (d) Calibration curves for building nomograms predicting 1, 3, and 5-year survival rates.

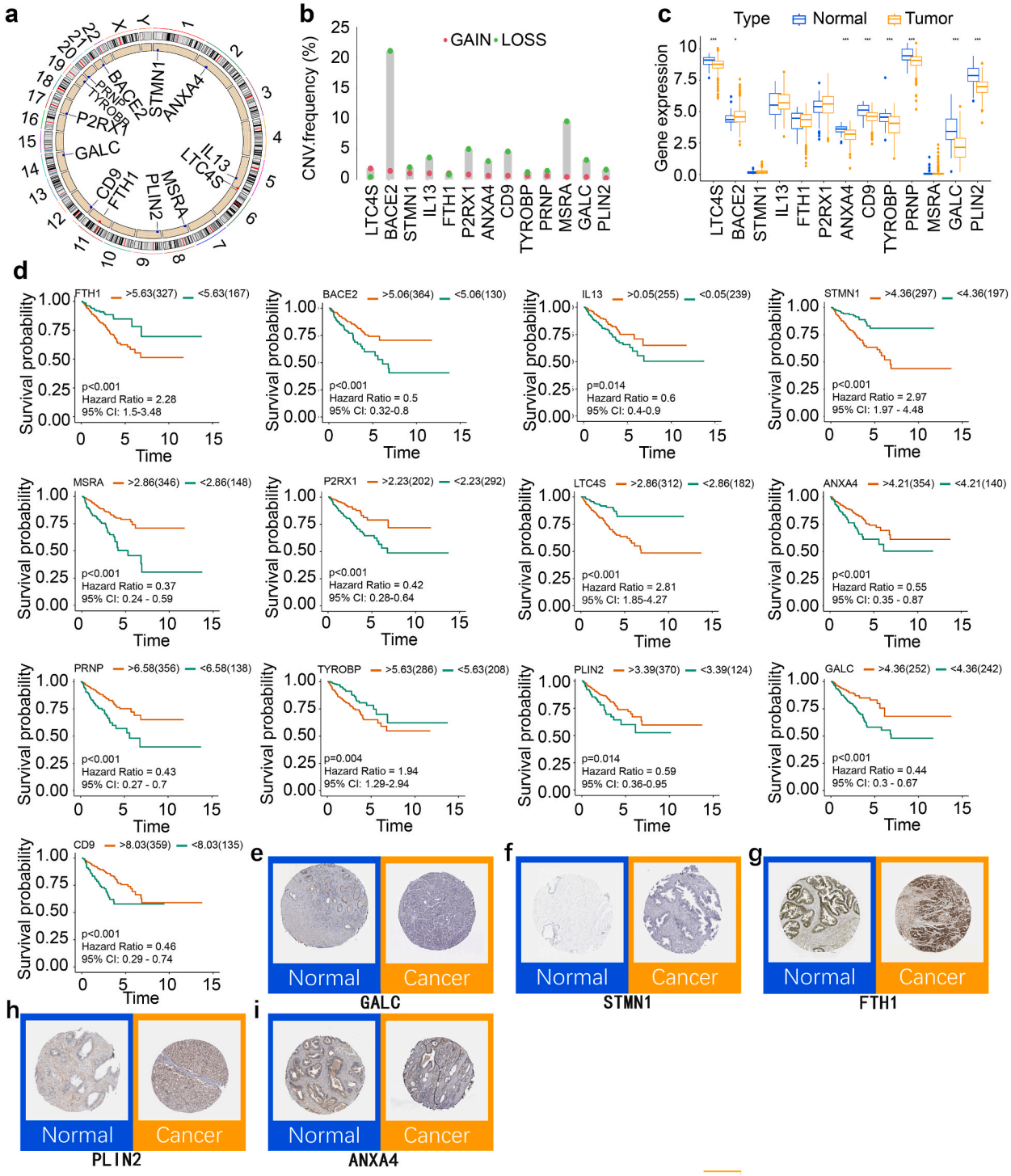

Fig. 6. Genetic variations of MCMGS gene features. (a) Chromosomal locations of CNV alterations in MCMGS gene features. (b) CNV alterations in MCMGS gene features. (c) Differential expression of MCMGS gene features in normal and tumor tissues. (d) Detailed analyses of survival curves for each MCMGS gene feature, classified by high- and low-expression groups. *$p < 0.05$; ***$p < 0.001$; ns, no statistical significance. Immunohistochemical analysis of MCMGS gene features. (e)–(i) Protein expression levels of GALC, STMN1, PLIN2, FTH1, ANXA4, and other genes in normal and tumor tissues.

3.6. Genetic variation and immunohistochemical analysis of MCMGS signature genes

To examine the overall expression of MCMGS feature genes in PRAD patients, we first analyzed the gene expression levels and identified altered CNV chromosomal locations, as depicted in Fig. 6a. We observed widespread CNV alterations in the MCMGS feature genes, with a majority of patients exhibiting decreased copy numbers (Fig. 6b). Furthermore, we analyzed mRNA expression levels of MCMGS feature genes among PRAD samples. Specifically, tumor tissues showed downregulated expression of FTH1, MSRA, ANXA4, PLIN2, CD9, P2RX1, and PRNP (all $p < 0.05$) and upregulated expression of STMN1 ($p < 0.05$) (Fig. 6c). We discovered that all of the MCMGS feature genes were linked to PRAD prognosis when stratified based on high and low expression (Fig. 6d).

To explore potential differences in protein expression levels of ten MCMGS signature genes (CD9, TYROBP, GALC, STMN1, PLIN2, FTH1, PRNP, MSRA, BACE2, ANXA4), we collected IHC-stained images from the HPA database, including samples from PRAD and benign prostatic hyperplasia tissues. We aimed to examine any possible variations in protein expression levels between these two sample types. Compared to normal samples, differential protein expression levels of the ten MCMGS feature genes were observed in PRAD samples, further supporting our findings (Fig. 5e–i).

3.7. Functional enrichment analysis of MCMGS-related genes

We conducted a functional enrichment analysis to identify the basic mechanisms and biological activities that contribute to the risk model's predictive abilities. We found 81 and 69 positively and negatively correlated genes, respectively, between the high- and low-risk groups in the TCGA cohort utilizing the "limma" package in R with filtering criteria of FDR <0.05 and $|\log2FC| \geq 1$. GO and KEGG enrichment analyses were performed on the selected genes using the "ClusterProfiler" tool.

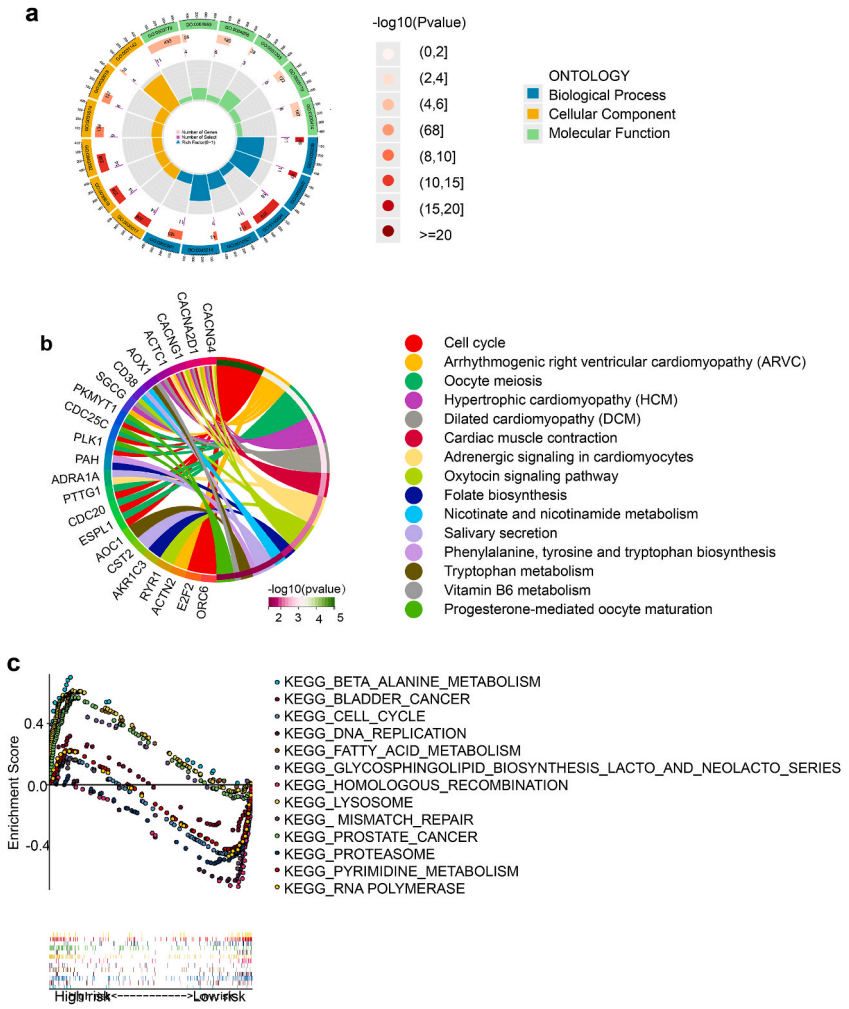

Fig. 7. The MCMGS was analyzed via functional enrichment analyses. KEGG and GO enrichment analyses (Figure a, b) were performed to explore the associated biological pathways and functional annotations. Additionally, GSVA analysis (Figure c) was carried out to assess the gene set variation between the high- and low-risk groups.

The GO analysis results illustrated that these genes were predominantly implicated in cellular processes, specifically mitotic cell division. The biological processes included non-membrane-bound organelle assembly, sister chromatid separation, chromosome segregation, nuclear chromosome segregation, mitotic nuclear division, organelle fission, and nuclear division. Cellular components (CC) mainly involved spindle, contractile fiber, centromeric region of chromosome, chromosomal region, and microtubule, among others. Molecular functions (MF) primarily included microtubule binding (Fig. 7a). The findings of KEGG analysis also revealed the enrichment of these genes in the cell cycle, oocyte meiosis, folate biosynthesis, nicotinate, and nicotinamide metabolism, and other cellular growth, death, coenzyme, and vitamin metabolism-related pathways (Fig. 7b).

The molecular mechanisms linked to these genes were investigated via GSEA. Notably, the enrichment pathways observed in the high-risk group encompassed fatty acid metabolism, beta-alanine metabolism, lysosome, prostate cancer, and glycosphingolipid biosynthesis lacto and neolacto series. In contrast, the enrichment pathways observed in the low-risk group primarily included homologous recombination, cell cycle, mismatch repair, pyrimidine metabolism, DNA replication, RNA polymerase, proteasome, and

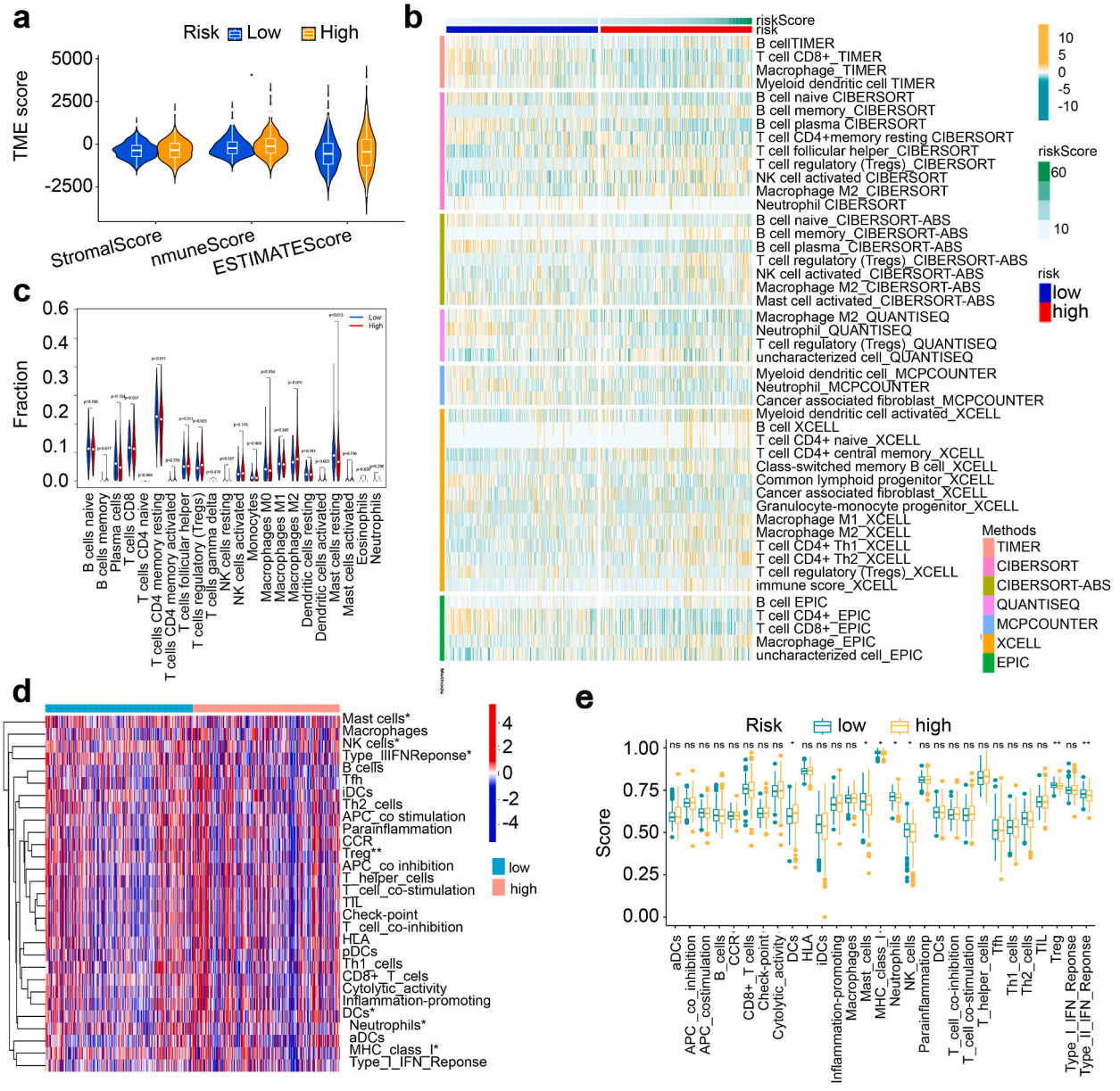

Fig. 8. The MCMGS risk score was utilized to predict tumor microenvironment and immune cell infiltration, as demonstrated by (a) Tumor microenvironment (TME) components predicted by the MCMGS risk score. (b) Immune cell correlation heatmap based on several different algorithms. (c) Relative abundance distribution of 22 tumor-infiltrating immune cells. (d) Expression and correlation analysis of immune cell populations. (e) Immune function scores based on MCMGS risk score.

bladder cancer (Fig. 7c).

3.8. MCMGS is associated with immune cell infiltration in TME

Variations in immune cell composition contribute to the diversity of immune responses. The role of Mast cells in anti-tumor immunity and their association with prognosis through immune infiltration in the tumor microenvironment (TME) remains unclear. For TCGA PRAD patients, we calculated ESTIMATE, immune, and stromal scores utilizing the ESTIMATE algorithm. Notably, immune scores were substantially greater in the high-risk group ($P < 0.05$), indicating increased overall immune level and immunogenicity in the TME (Fig. 8a). Immune cell correlation heatmaps generated using EPIC, XCEEL, MCPCOUNTER, QUANTISEQ, CIBERSORT-ABS, CIBERSORT, and TIMER algorithms exhibited augmented infiltration of Mast cell-related immune cells, regulatory T cells (Tregs), and M2 macrophages, in the high-risk group. Conversely, the low-risk category exhibited greater infiltration of $CD8^+$ T cells, macrophages, immature B cells, and neutrophils (Fig. 8b).

In the TCGA PRAD cohort, the CIBERSORT method was applied to analyze the distribution and association of 22 different types of tumor-infiltrating immune cells (TIICs). The low-risk category showed considerably greater infiltration levels of memory resting CD4 T cells, activated dendritic cells (DCs), and resting mast cells as opposed to the high-risk category. However, there were considerably increased Tregs in the high-risk group in contrast with those in the low-risk group (Fig. 8c).

The MCMGS risk score model demonstrates the ability to classify distinct immune subtypes, which may have implications for immunotherapy response. Variations in immune cell infiltration can influence immune function. Notably, we observed that the low-risk group had a higher abundance of neutrophils, MHC class I, mast cells, Mast cells, regulators, and type II IFN response, with their expression levels displaying an inverse link to the risk score (Fig. 8d and e).

3.9. TMB analysis

Using the map tools algorithm on TCGA PRAD data, we evaluated somatic mutation spectra across various risk categories. Increased mutation rates in the 15 most commonly mutated genes were observed in both high-and low-risk groups (Supplementary Fig. 2a). The frequency of mutations was greater (64.84 %) in the high-risk group contrasted with the low-risk group (43.39 %). In the high-risk group, mutations were more prevalent in SPOP (14 %), TP53 (12 %), and TTN (11 %), whereas in the low-risk group, these mutation rates were 9 %, 7 %, and 9 %, respectively. Importantly, Tumor mutational burden (TMB) was considerably greater in the high-risk group relative to the low-risk group ($P < 0.05$) (Supplementary Fig. 2b). The low-risk group with low TMB had the superior PFS, as shown by the survival analysis ($P < 0.05$) (Supplementary Fig. 2c). As per the median TMB and risk values, we divided patients into four categories (L-TMB + Low-risk, L-TMB + High-risk, H-TMB + Low-risk, and H-TMB + High-risk), and discovered that overall survival (OS) was highest for individuals with low TMB and low risk and lowest for those with high TMB and high risk (Supplementary Fig. 2d).

3.10. Evaluation of MCMGS risk scores to predict immunotherapy response

Immune checkpoint inhibitors (ICIs) have shown effectiveness in tumor therapy. Mast cells, key immune cells with potential roles in prostate cancer immunotherapy, are promising therapeutic targets. We assessed the predictive capability of MCMGS for response to ICI in PRAD. Notably, 14 immune checkpoint genes (ICG) showed substantial upregulation in the high-risk group, whereas only six ICGs exhibited upregulation in the low-risk group (Fig. 9a). The BEST database (https://rookieutopia.com/) was used to analyze immune modulator distribution in ten datasets and found a positive correlation between most immune modulators and MCMGS genes (Fig. 9b). Targeted therapy against these upregulated immune checkpoint genes may benefit patients with this tumor subtype. Analysis of the TCIA database predicted immune-based therapy responsiveness based on IPS, indicating immunogenicity. In Fig. 9c–f, we observed significantly higher Immune Phenotype Score (IPS) values in the low-risk group compared to the high-risk group across different immune subgroups, including those negative for CTLA-4 and PD-1, positive for CTLA-4 and negative for PD-1, and negative for CTLA-4 and positive for PD-1 ($p < 0.05$). These findings suggest that patients in the low-risk group may respond better to immunotherapy.

Next, we investigated the association between MCMGS scores and therapeutic benefits in an external cohort (GSE126044) of patients who were treated with immunotherapy. The high-risk patients displayed a stronger immune response against PD-L1 based on MCMGS scores, and the ROC curve confirmed MCMGS's effectiveness in predicting immunotherapy response (Fig. 9g). These findings collectively suggest that MCMGS can be a valuable tool for determining how PRAD patients will respond to ICIs.

3.11. Screening and analysis of drug sensitivity for small-molecule drugs

We employed the pRRophetic package to screen potential therapeutic agents for PRAD treatment, aiming to evaluate their effectiveness. Specifically, we examined six widely used antitumor drugs and examined the difference in IC50 between the high- and low-risk groups. Docetaxel, niraparib, oxaliplatin, cabozantinib, vincristine, and dactylitis all showed greater IC50 values (the dose needed to suppress cell growth by 50 %) in the high-risk group as opposed to the low-risk group (Fig. 9h–m), showing increased drug sensitivity in the low-risk group. These results lead to the assumption that risk scores serve as a stratification tool for achieving optimal treatment outcomes by providing insight into the likelihood that an individual would respond favorably to a certain drug.

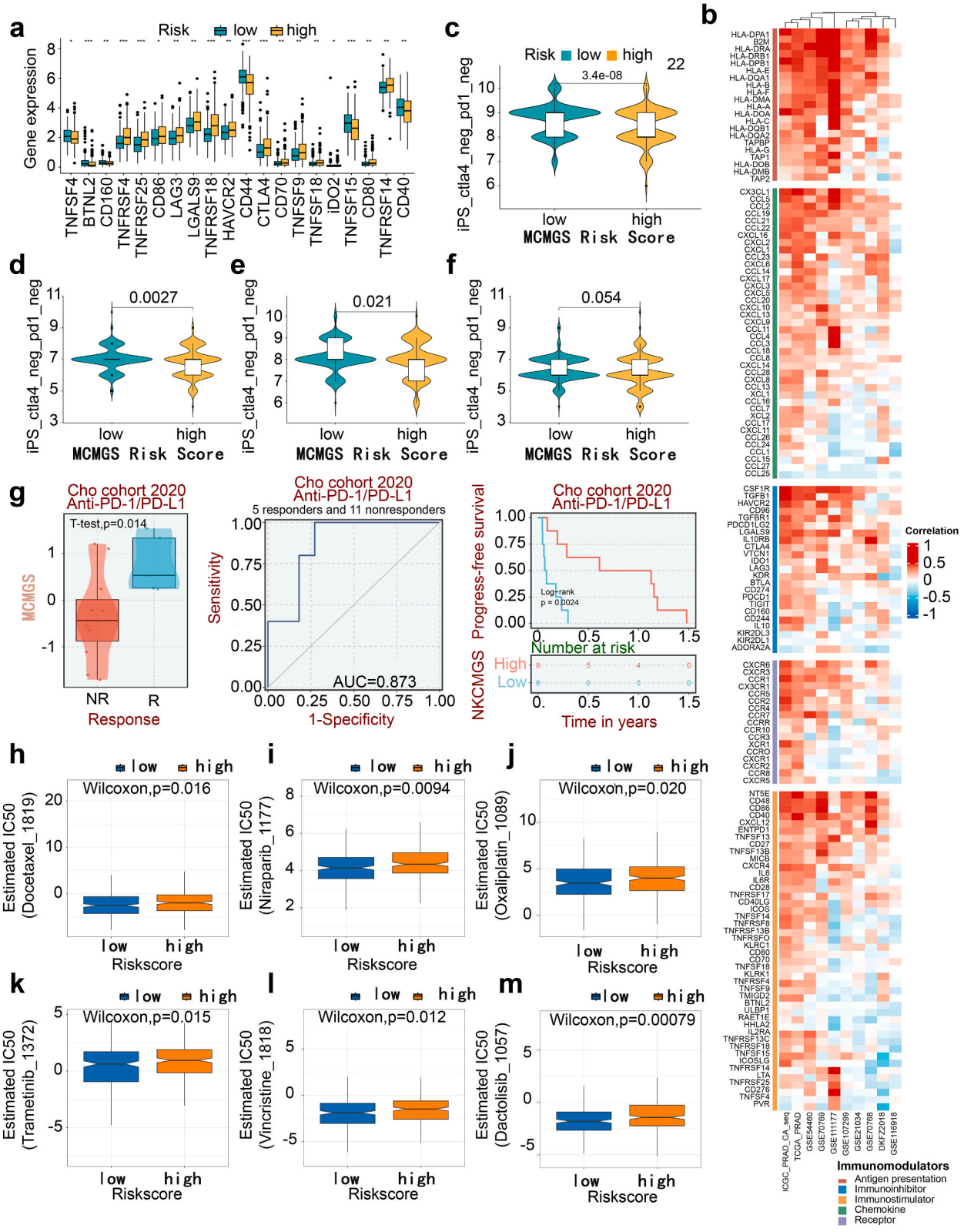

(caption on next page)

Fig. 9. Evaluation of MCMGS risk score in predicting immunotherapy response. (a) Variations in gene expression of immune checkpoints between high- and low-risk groups. (b) Heatmap displaying immune checkpoint expression across various datasets (ICGC-PRAD, TCGA, GSE54460, GSE70769, GSE111177, GSE107229, GSE21034, GSE70768, DKFZ2018, and GSE116918). (c), (d), (e), (f) Predicting immunotherapy sensitivity using IPS score. (g) Evaluating MCMGS efficacy for anti-PD-L1 therapy in the GSE126044 cohort. Prediction of chemotherapy sensitivity by MCMGS signature. (h) Docetaxel, (i) Niraparib, (j) Oxaliplatin, (k) Cabozantinib, (l) Etoposide, and (m) Dactolisib IC50 values.

3.12. Pan-cancer analysis of MCMGS characterized genes

Our study repeatedly confirms the crucial value of the aforementioned 13 genes comprising the MCMGS in PRAD. However, to summarize the pan-cancer spectrum of these 13 genes, it is essential to investigate their involvement across various human malignancies, including expression profiles, predictive capabilities, methylation patterns, CNVs, and SNVs. Firstly, we established survival profiles for the relevant genes by linking gene expression levels from TCGA with patient survival outcomes (Fig. 10a). Furthermore, we evaluated the gene expression in tumor tissue in comparison to that in healthy tissues in TCGA. We found that the expression of these 13 genes is generally upregulated in tumor tissues (Fig. 10b). In most cancers, these signature genes exhibit differential methylation compared to normal tissues; notably, we observed a tendency towards higher levels of methylation (Fig. 10c). Abundant CNV losses were observed in these genes across multiple tumor types (Fig. 10d). Single nucleotide variation (SNV) analysis revealed that the most prevalent mutation types among the 33 tumor types in TCGA were MCMGS missense mutations, with the highest frequency being single nucleotide polymorphisms. Among different SNV categories, C > T alterations have the highest frequency (Fig. 10e). Out of 480 patients across the 33 tumor types, GLAC showed the highest mutation frequency (Fig. 9f). Next, we conducted copy number variation analysis and summarized the proportion of homozygous and heterozygous mutations within MCMGS across the 33 tumor samples (Fig. 10g).

Expanding upon these findings, we further investigated the association between cancer-related pathway activity and the expression of NRGs. Remarkably, our results demonstrate that MCMGS exerts regulatory influence on diverse pathways in different tumor types, modulating the hormone AR and EMT pathways in PRAD patients (Fig. 10h). We investigated the correlation between MCMGS differential expression and drug sensitivity using the Cancer Therapeutics Response Portal and GDSC databases (Fig. 10i and j). This highlights the potential of our risk spectrum gene expression patterns as predictive factors for chemotherapeutic drug sensitivity in patients and as targets for future drug sensitization strategies.

3.13. Expression of MCMGS characterized genes in immune and molecular subtypes in PRAD

We examined the link between MCMGS and distinct immune and molecular subtypes by using the TISIDB database. We identified 12 genes, including FTH1, STMN1, GALC, BACE2, MSRA, ANXA4, PLIN2, CD9, LTC4S, TYROBP, P2RX1, and PRNP, that closely correlated with four distinct PCA immune subtypes: C1: wound healing subtype, C2: IFN-γ dominant subtype, C3: inflammatory subtype, C4: lymphocyte depleted subtype (Fig. 11a). Furthermore, we observed differential expression of these 12 genes across different molecular subtypes in PRAD; each gene exhibited significant variations in different molecular subtypes (Fig. 11b).

4. Discussion

PCA is the most prevalent malignant neoplasm and the second leading contributor to cancer-associated mortality in men worldwide [1]. After early radical treatment of PCA patients, further disease progression occurs after some time, primarily in the form of elevated biochemical indicators (PSA) and imaging progression. In this context, the criterion for biochemical recurrence is defined as two consecutive PSA $\geq$0.2 ng/ml on the premise of negative imaging. Biochemical recurrence is the earliest manifestation of disease recurrence. It is a decisive risk factor for distant metastasis and prostate-specific mortality in prostate cancer. Approximately 30 % of patients with biochemical recurrence will have distant metastases, and in the absence of a second treatment, 19–27 percent of patients may die during the first 10 years after being diagnosed with PCA [31,32]. Early identification of risk factors for disease progression and early intervention to prolong the time to disease progression will result in better overall survival. Post-radical treatment, the integration of multiple biomarkers into a cohesive model is essential for enhancing prognostic accuracy, evaluating immune responses, and predicting drug sensitivity. This integrated approach allows for a more nuanced understanding of patient outcomes and can guide personalized treatment strategies. This approach enables the development of personalized treatment plans, active monitoring of high-risk patients, and timely intervention in disease progression. These measures are essential for enhancing prognosis in patients with prostate cancer.

Mast cells within the tumor microenvironment (TME) are a subject of scientific debate, with their roles being tumor-specific and stage-dependent [33]. These cells have the potential to either support tumorigenesis through the promotion of inflammatory responses and angiogenesis, acting as a source of VEGF α, TGF-β, and CXCL8 [34], which are markers of poor prognosis, or to exert anti-tumor effects by releasing mediators that activate immune cells. The correlation between mast cells and tumor angiogenesis, along with their infiltration into cancer cells, has been strongly associated with adverse outcomes, suggesting a pro-tumor role for these cells. However, mast cells have also been reported to play a role in tumor suppression [14–17]. In the context of prostate cancer, mast cells have been linked to the invasiveness and metastatic potential of the tumor [21]. Notably, The modulation of mast cell quantity or functionality could potentially lead to improved therapeutic responses in prostate cancer [18]. The MCT subtype of mast cells is associated with unfavorable clinical outcomes, indicating a possible contribution to immune evasion and tumor progression [19]. In an innovative

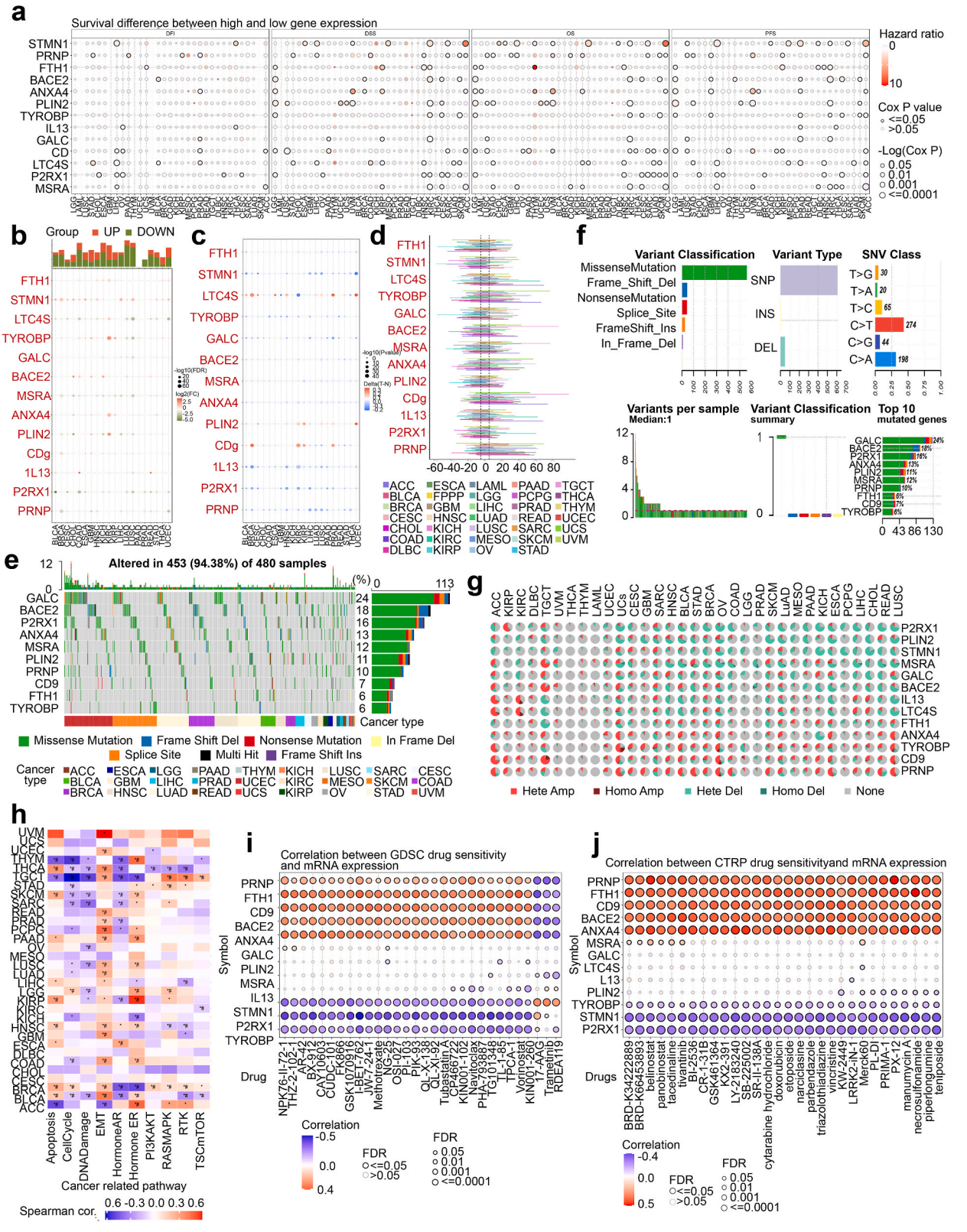

(caption on next page)

Fig. 10. Pan-cancer analysis of MCMGS signature genes. (a) Bubble plot showing the correlation between gene expression levels in the TCGA dataset and survival outcomes across different cancer patients. (b) Differential expression of relevant genes in pan-cancer. (c) Differences in tumor promoter methylation between pan-cancer and normal promoter methylation of relevant genes. (D) Copy number variation rates of relevant genes in pan-cancer. (e) (f) Classification and mutation frequency of MCMGS mutations in multiple tumors. (g) Expression of MCMGS signature genes in multiple tumors. (h) The relationship between GSVA scores of MCMGS signature genes and cancer-associated pathway activity in certain cancers is summarized in Figure. (i) (j) Correlation analysis between NRGs expression and chemotherapy drug sensitivity in CDRP and CDSC cohorts.

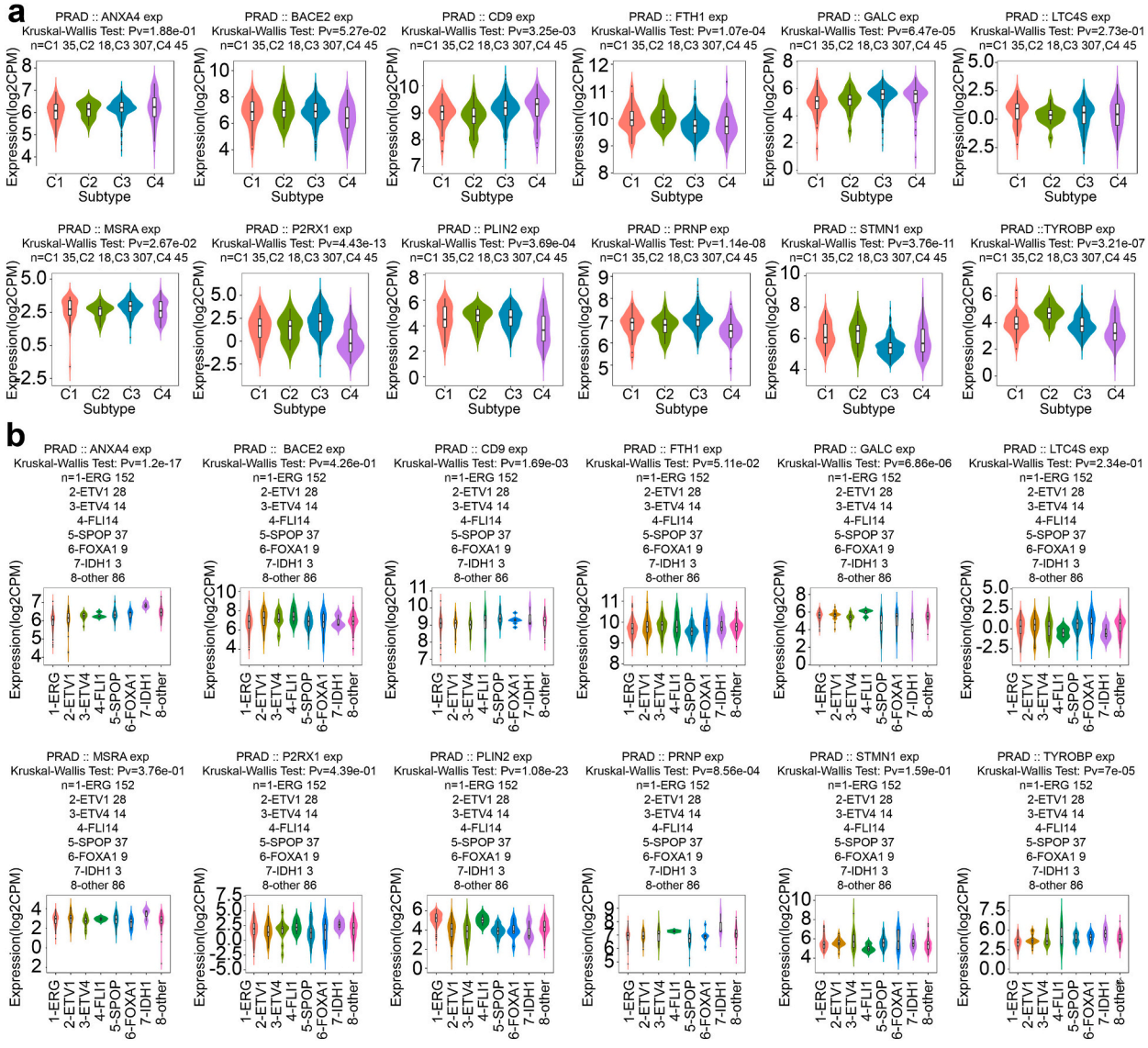

Fig. 11. Expression of MCMGS signature genes in immune and molecular subtypes of PRAD. (a) Expression levels of FTH1, STMN1, GALC, BACE2, MSRA, ANXA4, PLIN2, CD9, LTC4S, TYROBP, P2RX1, and PRNP in different immune subtypes of PRAD. (b) Differential expression of FTH1, STMN1, GALC, BACE2, MSRA, ANXA4, PLIN2, CD9, LTC4S, TYROBP, P2RX1, and PRNP in different molecular subtypes of PRAD.

study, Peng Song and colleagues employed single-cell RNA sequencing to predict the survival and treatment response of patients with lung adenocarcinoma (LUAD). They developed a seven-gene signature based on NK cell marker genes, which could assist in clinical decision-making and identify patients who may benefit from immunotherapy [24].The study capitalized on the advancements in scRNA technology, providing a powerful tool to explore tumor heterogeneity and distinct cellular subpopulations. Inspired by these developments, the researchers initially conducted single-cell sequencing using the GEO dataset, screening 168 Mast-cell-related genes in prostate cancer. These genes were found to be predominantly linked to immune features such as T-cell activation, mast cell activation, and immune response, as determined by KEGG and GO analyses. Subsequently, we conducted univariate analysis on the TCGA

PRAD dataset to identify genes associated with prognosis. A comprehensive evaluation of 101 combinations involving 10 machine learning algorithms led to the identification of the optimal model, which consisted of a combination of CoxBoost and RSF based on the highest C-index. This approach effectively reduced variable dimensionality, unveiled underlying patterns, and simplified and refined the model. Consequently, the established MCMGS model accurately predicts the prognosis and immune characteristics of PRAD patients. Thirteen characteristic genes MCMGS of Mast cell markers associated with the prognosis of prostate cancer were finally identified. These 13 MCMGS were FTH1, STMN1, LTC4S, TYROBP, GALC, BACE2, MSRA, ANXA4, PLIN2, CD9, IL13, P2RX1, and PRNP.

FTH1, as a 21 kDa subunit of the ferritin complex, minimizes DNA damage caused by reactive oxygen species (ROS) induced by ferrous iron (Fe2+) through its ferroxidase activity, which converts Fe2+ to ferric iron (Fe3+). This protective mechanism helps cancer cells avoid cell death [35]. FTH1 serves as a key regulator of iron metabolism and an essential factor in the inhibition of ferroptosis, closely related to the tumor immune microenvironment (TIME) [36]. In a glioblastoma mouse model, FTH1 affects the tumor infiltration of T cells, $CD8^+$ T cells, fibroblasts, and mast cells, influencing tumor growth, and may also affect human glioblastoma, which requires further experimental confirmation [37]. The interaction between FTH1 and miR-29a-5p plays a significant role in ferroptosis in prostate cancer [38].STMN1 (Stathmin1) is a regulatory protein involved in cytoskeleton and microtubule processes, showing significant upregulation in immunodeficient tumors. STMN1 has an oncogenic role in various cancers [39,40]. Overexpression of STMN1 in PCA implies higher tumor aggressiveness [41]. Our study indicates that STMN1 expression is associated with immune infiltration and adverse survival outcomes. This is consistent with the findings of Zhang et al. where STMN1 is related to immune regulation, DNA methylation, and m6A in hepatocellular carcinoma [42]. These findings emphasize the necessity of evaluating the involvement of STMN1 in immune regulation and its potential impact on clinical prognosis.LTC4S catalyzes the production of cysteinyl leukotrienes, which are pro-inflammatory mediators in inflammatory diseases. The expression of LTC4S is significantly correlated with the infiltration of typical adaptive immune cells, especially B cells, T cells, and mast cells [43,44]. The genes LTC4S, APPL2, AMD1, ALDH1A3, OAT, and TPD52 are upregulated in prostate cancer tissues of African American men, and these genes may have a potential role in the aggressiveness of prostate cancer in African American males [45]. The role of LTC4S in the aggression of prostate cancer requires further research.TYROBP (also known as DAP12) is a transmembrane signaling adapter protein that pairs with various receptors. It contains a cytosolic immunoreceptor tyrosine-based activation motif (ITAM) expressed in NK cells and myeloid cells. Additionally, it may involve members of the immunoglobulin superfamily (TREM-1, -2, and -3) [46]. YTS cells, modified with anti-PSCA-DAP12 CAR, show highly specific lysis of PSCA-positive target cells from PCA, bladder cancer, and glioblastoma. In contrast, PSCA-negative cancer cells are unaffected. These findings suggest that DAP12-based CAR is a promising tool for adjunctive immunotherapy [47].GALC (β-galactosidase) is a lysosomal enzyme that removes β-galactose from β-galactosides, leading to the formation of the tumor suppressor metabolite ceramide, which is a tumor suppressor metabolite. Recent observations suggest that GALC may have opposite effects on tumor growth by acting as a tumor suppressor or an oncogenic enzyme [48]. GALC induces tumorigenicity in colorectal cancer through senescent fibroblasts [49]. Targeted correction of the BACE2/TMEM38B axis leads to the depletion of intracellular calcium release and inhibits tumor progression. BACE2 shows promise as a potential therapeutic target for ocular melanoma based on certain findings [50]. Its role in prostate cancer still requires further research.The methionine sulfoxide reductase (Methionine sulfoxide reductase, MSRA) encoded by the MSRA gene is a key factor in protecting proteins from oxidation and acts as a scavenger of reactive oxygen species (ROS) [51]. Its tumor suppressor role is stronger in lung squamous cell carcinoma and adenocarcinoma than in adjacent normal tissue [52]. Although MSRA has not been studied in prostate cancer, its differential expression was found in this study, and its association with prostate cancer can be further confirmed in future research.Annexin A4 (ANXA4) is a protein that may bind to phospholipids and calcium ions, an important factor in regulating membrane permeability and processes such as cell growth, apoptosis, tumor invasion, and antitumor treatment, including extracellular matrix, cell adhesion molecules, and cell signaling [53]. Pan-cancer analysis has found that ANXA4 has the potential to be a new clinical prognostic marker and therapeutic target in various cancer types [54]. ANXA4 is highly expressed in various tumors, and increased expression and nuclear translocation of ANXA4 are associated with disease progression in colorectal and ovarian plasma cell-like carcinoma [55,56]. Interestingly, our results suggest that ANXA4 expression is reduced in tumor tissue, which is consistent with previous studies [57], and its expression level may be associated with the progression of prostate cancer, and the specific mechanism of action is worth further research.PLIN2 belongs to the PAT family and is involved in the regulation of lipid droplet formation and degradation. It is mainly expressed in adipose and steroidogenic cells, where lipid droplets play an important role in ketone body metabolism [58]. Upregulation of PLIN2 is correlated with poor prognosis in patients with clear cell renal cell carcinoma, and knockdown of PLIN2 enhances cancer cell proliferation and accelerates the invasion and migration of cancer cells, which is a recent finding [59]. Clinically, PLIN2 is expressed at higher levels in primary prostate cancer with higher Gleason scores and compared to dedifferentiated prostate cancer [60].CD9, together with E-cadherin, serves as a biomarker for renal cell carcinoma (RCC), helping not only in differentiation but also in predicting the metastatic tendency of RCC [61]. Studies have shown that patients with advanced metastatic PCA have increased double positivity for CD9 and prostate-specific membrane antigen (PSMA) in plasma-derived circulating vesicles. On the other hand, in patients with limited PCA, double positivity for CD9 and CD63 small extracellular vesicles (S-EVs) is significantly enhanced [62].IL13 is an immunomodulatory factor with regulatory functions in inflammation and immune responses. It is produced by Th2 cells, NKT cells, mast cells (MC), and basophils [63]. Compared with adjacent normal tissue, upregulation of IL-13 expression is observed in COAD tissue. Furthermore, a study involving 241 patients with CRC found that serum IL-13 levels were significantly lower in patients with advanced cancer, which was associated with a poorer prognosis [51]. During the resolution of inflammation, regulatory T (Treg) cells secrete IL13, promoting the efflux of macrophages and enhancing the engulfment of apoptotic cells [64]. In this study, IL-13 is relatively highly expressed in tumors, and Riaz Jannoo et al. found that IL-13 Rα2 cell surface receptors are highly expressed in prostate cancer [65].P2RX1, under the regulation of interleukin-13 (IL-13), promotes the efflux of macrophages and enhances the engulfment

of apoptotic cells [32]. Wareham et al. [66] found that LAD2 cells and human pulmonary mast cells both have functional P2RX1. In our study, P2RX1 is associated with cell death and inflammatory responses and may play a role in the immune regulation and cell death of tumors. However, to date, there is a lack of published research investigating the role of P2RX1 in prostate cancer, providing a potential avenue for future research.PRNP, also known as CD230, encodes the PrP protein primarily found in the nervous system but expressed in various tissues. In this study, PRNP expression is downregulated in tumor tissue. Previous research has shown that decreased PRNP expression in prostate cancer is significantly associated with biochemical recurrence-free survival in PCA patients [67]. In breast cancer, PRNP is significantly downregulated and may be involved in ROS-mediated ferroptosis, a potential new therapeutic target for chemotherapy and immunotherapy [68]. PRNP can serve as a potential biomarker for stratification of colorectal cancer patients [69]. PRNP shows promise as a potential prognostic factor in gastric cancer (GC) patients [70]. These data confirm that MCMGS is related to tumor progression, providing a target gene for future experimental validation, which may provide compelling evidence for the molecular mechanisms behind the occurrence and development of PCA.

We found that the risk profile of MCMGS independently functioned as a prognostic factor for PCA, which is important in clinical practice. First, we constructed prognostic models, KM survival curves, ROC curves, and calibration curves utilizing the 13 gene expression levels identified by machine learning algorithms. The evaluation of these features associated with MCMGS in PRAD patients revealed that low-risk patients had a superior prognosis as opposed to those at high risk and could serve as independent prognostic factors. Our MCMGS-associated features model exhibited better AUC values than age, T-stage, Gleason score, and PSA value, indicating improved predictive performance. Furthermore, external validation across all five datasets consistently demonstrated the model's robust potential for predicting PRAD patients' prognoses. Furthermore, we collected and compared 10 published signatures comprising different combinations of functional genes. Unfortunately, as of yet, only a few of these signatures have been translated into actual clinical use. Moreover, several models exhibited satisfactory performance solely on the training dataset but performed poorly when applied to the validation dataset, indicating limited generalizability. Notably, the MCMGS signature outperformed nearly all other signatures, as evidenced by its higher AUC value. This suggests that our MCMGS signature, derived from feature gene selection and statistical prediction using a well-fitted model employing two combined machine-learning algorithms, is both stable and promising. Consequently, our newly developed column line graphs, based on this signature, hold the potential for enhancing the process of making decisions in clinical settings and guiding the development of therapeutic strategies.

We performed further KEGG and GO enrichment analyses to examine the molecular mechanisms of MCMGS on the onset and progression of PCA. Through these analyses, we discovered that the relevant genes were primarily linked to the cell growth cycle, cell division, and metabolic pathway. This led to the hypothesis that MCMGS may play a role in PCA progression. It is possible that abnormalities in the cell cycle, which are strongly related to the onset and progression of tumors, lead to the dismal prognosis that was observed in high-risk patients [71]. Recent research on PCA has shown that the tumor microenvironment performs an essential role in the onset and progression of this disease [72]. Our MCMGS model takes into account both the tumor microenvironment (TME) and tumor heterogeneity. Through analysis using seven algorithms (EPIC, QUANTISEQ, MCPCOUNTER, CIBERSORT-ABS, XCEEL, CIBERSORT, and TIMER), we discovered that the low-risk patients exhibited a greater abundance of $CD8^+$ T cells, macrophages, B-cell naïve, neutrophils, and other immune cell types. Additionally, the low-risk group had elevated levels of immune cell infiltration, as measured by CD4 memory quiescent T cells, DC activation, and quiescent mast cells, as opposed to the high-risk group, as determined by an analysis of 22 TIICs profiles in the TCGA PRAD cohort. Conversely, a lower level of immune cell infiltration was observed in the high-risk group. Notably, an upregulation of M2-like macrophages and Tregs was observed in the high-risk group. It was shown that males who had a high number of M2 macrophages present in thein the prostate tumor environment were at an elevated risk of dying from PCA. According to the findings of Erlandsson et al. this provides support for the hypothesis that M2 macrophages can work in conjunction with other variables, like T suppressor cells, to create an immunosuppressive environment [73]. Aggregation of circulating or tumor-infiltrating Tregs in cancer patients tends to correlate with poor prognosis [74]. The findings of the aforementioned investigation are consistent with this study. As per the data, reduced immune cell infiltration levels likely make it easier for tumor cells to evade the immune system and facilitate the progression of tumors. The worse prognosis that was reported in the PRAD patients who were in the high-risk category may be partly explained by these characteristics.

TMB refers to the accumulation of mutations in somatic cells that lead to the production of neoantigens that trigger anti-tumor immune responses. New research points to TMB as a reliable biological marker for predicting the response to immunotherapy. Notably, the high-risk group was found to have higher levels of TMB than the low-risk group. We found that 14 ICGs were remarkably upregulated in the high-risk group (TNFRSF4, TNFRSF25, CD86, LAG3, LGALS9, TNFRSF18, HAVCR2, CTLA4, CD70, TNFSF9, TNFSF18, IDO2, CD80, TNFRSF14). Markedly, CD80 plays a crucial role by binding to either CD28 or CTLA4, thereby activating T cell costimulation or initiating T cell costimulation, correspondingly. These findings highlight the potential of ICI therapy as an effective approach to tumor treatment [75]. We also examined the cohort receiving immunotherapy (Cho cohort 2020) using the BEST database to examine the correlation between MCMGS score and response to immunotherapy and discovered that the immune response against PD-L1 was stronger in high-risk patients. Furthermore, the ROC curve verified the validity of MCMGS in predicting responsiveness to immunotherapy. In conclusion, these results indicate a higher likelihood of immunotherapy benefits for high-risk patients. MCMGS shows promise as a reliable biological marker for predicting the outcome of immunotherapy, and more validation is required before making any firm conclusions. We examined a series of chemotherapeutic and targeted medications with varying risk profiles to discover appropriate pharmaceuticals to satisfy the demands of individualized therapy and enhance the prognosis of PRAD patients. The results showed that some commonly used antitumor drugs such as docetaxel, niraparib, oxaliplatin, trametinib, vincristine, and Dactolisib were more sensitive to low-risk patients. Therefore, these drugs are expected to be used as effective anti-tumor treatments for patients with low expression of MCMGS.

Our study identified these genes as important biomarkers for PRAD. To evaluate the potential use of the 13 MCMGS signature genes

in other tumor types, we performed a comprehensive pan-cancer analysis. Our results revealed diverse roles of these genes in human cancers, including altered expression profiles, predictive values, methylation profiles, and CNV and SNV alterations. Furthermore, there was an increase in the protein expression level of these genes in PRAD samples compared to controls, suggesting a role for them in cancer onset and progression. Clinical use of the MCMGS signature genes as diagnostic and prognostic biological markers for cancer is feasible. They can serve as diagnostic markers for various cancers due to their differential expression in tumor tissues. Additionally, they show promise as prognostic indicators or therapeutic targets based on their association with patient survival and CNV modification. These results enhance our understanding of the pan-cancer profile of MCMGS-characterized genes and their clinical significance. Nonetheless, more research is required to verify our results and understand the molecular mechanism behind the involvement of these genes in cancer onset and progression.

In this study, we developed Mast cell-related prognostic features for prostate cancer using single-cell sequencing and machine-learning algorithms. We validated these features using multiple datasets and compared them with 10 previously published prognostic markers. Our results demonstrated that the MCMGS risk score outperformed existing prognostic markers, including PSA, T stage, and Gleason score, as indicated by a higher AUC value and better discrimination capability in predicting patient outcomes. However, there are limitations to consider. The data relied on online databases, mainly representing Western populations, introducing potential selection bias and impacting model robustness. Prospective studies, as well as ex vivo and in vivo trials, are needed to explore immunotherapy efficacy in patients with different risk profiles and uncover the underlying molecular mechanisms in prostate cancer.

5. Conclusion

In conclusion, we have developed a powerful feature based on 13 gene markers associated with Mast cells using advanced bioinformatics and machine learning techniques. These features serve as highly effective predictors of prognosis and treatment response in PRAD patients. They act as robust prognostic indicators for personalized prediction in clinical decision-making and aid in identifying individuals who are suitable candidates for immunotherapy.

Funding

This study was supported by the Key Project of Natural Science Foundation of Xinjiang Uygur Autonomous Region (Number: 2022D01D39), Xinjiang Uygur Autonomous Region Tianshan Talent Youth Top-notch Project (Number: 2022TSYCCX0026), National Science and Nature Fund (Number: 82360476) and Xinjiang Uygur Autonomous Region Natural Science Outstanding Youth Programme (Number: 2023D01E05).

Data availability statement

The findings presented in this study are based on data sourced from various databases, including the TCGA research network (https://www.cancer.gov/tcga) and the GEO database (https://www.ncbi.nlm.nih.gov/geo/) with accessions GSE46602, GSE70770, and GSE193337. The PRAD-CA and PRAD-FR data were obtained from the International Cancer Genome Consortium (ICGC, https://dcc.icgc.org/) database. The DKFZ dataset was retrieved from cBioPortal (https://www.cbioportal.org/), while the E-MTAB-6128 dataset was obtained from the ArrayExpress database (www.ebi.ac.uk/biostudies/arrayexpress).

Consent for publication

Not Applicable.

CRediT authorship contribution statement

Abudukeyoumu Maimaitiyiming: Writing – review & editing, Writing – original draft, Visualization, Validation, Supervision, Software, Methodology, Investigation, Conceptualization. **Hengqing An:** Writing – review & editing, Visualization, Validation, Funding acquisition. **Chen Xing:** Writing – review & editing, Formal analysis, Data curation. **Xiaodong Li:** Formal analysis, Data curation. **Zhao Li:** Formal analysis, Data curation. **Junbo Bai:** Formal analysis, Data curation. **Cheng Luo:** Formal analysis, Data curation. **Tao Zhuo:** Formal analysis, Data curation. **Xin Huang:** Formal analysis, Data curation. **Aierpati Maimaiti:** Formal analysis, Data curation. **Abudushalamu Aikemu:** Data curation. **Yujie Wang:** Visualization, Validation, Supervision, Investigation.

Declaration of competing interest

The authors declare that they have no known competing financial interests or personal relationships that could have appeared to influence the work reported in this paper.

Acknowledgments

We acknowledge and appreciate the contributors of the public databases utilized in this study. We are grateful to Figdraw (https://www.figdraw.com/) for offering a platform that enabled us to craft various flowchart materials.

Appendix A. Supplementary data

Supplementary data to this article can be found online at https://doi.org/10.1016/j.heliyon.2024.e35157.

References

[1] G. Francolini, B. Detti, V. Di Cataldo, P. Garlatti, M. Aquilano, A. Allegra, S. Lucidi, C. Cerbai, L.P. Ciccone, V. Salvestrini, G. Stocchi, B. Guerrieri, L. Visani, M. Loi, I. Desideri, M. Mangoni, I. Meattini, L. Livi, Study protocol and preliminary results from a mono-centric cohort within a trial testing stereotactic body radiotherapy and abiraterone (ARTO-NCT03449719), Radiol. Med. 127 (2022) 912–918, https://doi.org/10.1007/s11547-022-01511-7.

[2] F. Bray, M. Laversanne, H. Sung, J. Ferlay, R.L. Siegel, I. Soerjomataram, A. Jemal, Global cancer statistics 2022: GLOBOCAN estimates of incidence and mortality worldwide for 36 cancers in 185 countries, Ca - Cancer J. Clin. (2024), https://doi.org/10.3322/caac.21834.

[3] M.R. Cooperberg, P.R. Carroll, Trends in management for patients with localized prostate cancer, 1990-2013, JAMA 314 (2015) 80, https://doi.org/10.1001/jama.2015.6036.

[4] A.N. Boettcher, A. Usman, A. Morgans, D.J. VanderWeele, J. Sosman, J.D. Wu, Past, current, and future of immunotherapies for prostate cancer, Front. Oncol. 9 (2019) 884, https://doi.org/10.3389/fonc.2019.00884.

[5] N.D. Shore, Chemotherapy for prostate cancer: when should a urologist refer a patient to a medical oncologist? Prostate Cancer Prostatic Dis. 16 (2013) 1–6, https://doi.org/10.1038/pcan.2012.23.

[6] C.J. Paller, E.S. Antonarakis, Management of biochemically recurrent prostate cancer after local therapy: evolving standards of care and new directions, Clin. Adv. Hematol. Oncol. 11 (2013) 14–23.

[7] D. Hanahan, L.M. Coussens, Accessories to the crime: functions of cells recruited to the tumor microenvironment, Cancer Cell 21 (2012) 309–322, https://doi.org/10.1016/j.ccr.2012.02.022.

[8] M. Binnewies, E.W. Roberts, K. Kersten, V. Chan, D.F. Fearon, M. Merad, L.M. Coussens, D.I. Gabrilovich, S. Ostrand-Rosenberg, C.C. Hedrick, R.H. Vonderheide, M.J. Pittet, R.K. Jain, W. Zou, T.K. Howcroft, E.C. Woodhouse, R.A. Weinberg, M.F. Krummel, Understanding the tumor immune microenvironment (TIME) for effective therapy, Nat. Med. 24 (2018) 541–550, https://doi.org/10.1038/s41591-018-0014-x.

[9] H.-R. Cha, J.H. Lee, S. Ponnazhagan, Revisiting immunotherapy: a focus on prostate cancer, Cancer Res. 80 (2020) 1615–1623, https://doi.org/10.1158/0008-5472.CAN-19-2948.

[10] K. Mehta, K. Patel, R.A. Parikh, Immunotherapy in genitourinary malignancies, J. Hematol. Oncol. 10 (2017) 95, https://doi.org/10.1186/s13045-017-0457-4.

[11] S.M.T. Nguyen, C.P. Rupprecht, A. Haque, D. Pattanaik, J. Yusin, G. Krishnaswamy, Mechanisms governing anaphylaxis: inflammatory cells, mediators, endothelial gap junctions and beyond, Int. J. Mol. Sci. 22 (2021) 7785, https://doi.org/10.3390/ijms22157785.

[12] D. Ribatti, R. Tamma, E. Crivellato, Cross talk between natural killer cells and mast cells in tumor angiogenesis, Inflamm. Res. 68 (2019) 19–23, https://doi.org/10.1007/s00011-018-1181-4.

[13] K. Nagata, C. Nishiyama, IL-10 in mast cell-mediated immune responses: anti-inflammatory and proinflammatory roles, Int. J. Mol. Sci. 22 (2021) 4972, https://doi.org/10.3390/ijms22094972.

[14] H. Liu, Y. Yang, Identification of mast cell-based molecular subtypes and a predictive signature in clear cell renal cell carcinoma, Front. Mol. Biosci. 8 (2021) 719982, https://doi.org/10.3389/fmolb.2021.719982.

[15] L. Zhang, J. Pan, Z. Wang, C. Yang, W. Chen, J. Jiang, Z. Zheng, F. Jia, Y. Zhang, J. Jiang, K. Su, G. Ren, J. Huang, Multi-omics profiling suggesting intratumoral mast cells as predictive index of breast cancer lung metastasis, Front. Oncol. 11 (2022) 788778, https://doi.org/10.3389/fonc.2021.788778.

[16] M. Okano, M. Oshi, A.L. Butash, E. Katsuta, K. Tachibana, K. Saito, H. Okayama, X. Peng, L. Yan, K. Kono, T. Ohtake, K. Takabe, Triple-negative breast cancer with high levels of annexin A1 expression is associated with mast cell infiltration, inflammation, and angiogenesis, Int. J. Mol. Sci. 20 (2019) 4197, https://doi.org/10.3390/ijms20174197.

[17] R. Chen, W. Wu, T. Liu, Y. Zhao, Y. Wang, H. Zhang, Z. Wang, Z. Dai, X. Zhou, P. Luo, J. Zhang, Z. Liu, L.-Y. Zhang, Q. Cheng, Large-scale bulk RNA-seq analysis defines immune evasion mechanism related to mast cell in gliomas, Front. Immunol. 13 (2022) 914001, https://doi.org/10.3389/fimmu.2022.914001.

[18] H. Hempel Sullivan, C.M. Heaphy, I. Kulac, N. Cuka, J. Lu, J.R. Barber, A.M. De Marzo, T.L. Lotan, C.E. Joshu, K.S. Sfanos, High extratumoral mast cell counts are associated with a higher risk of adverse prostate cancer outcomes, Cancer Epidemiol. Biomarkers Prev. 29 (2020) 668–675, https://doi.org/10.1158/1055-9965.EPI-19-0962.

[19] H. Hempel Sullivan, J.P. Maynard, C.M. Heaphy, J. Lu, A.M. De Marzo, T.L. Lotan, C.E. Joshu, K.S. Sfanos, Differential mast cell phenotypes in benign versus cancer tissues and prostate cancer oncologic outcomes, J. Pathol. 253 (2021) 415–426, https://doi.org/10.1002/path.5606.

[20] B.A. Pereira, N.L. Lister, K. Hashimoto, L. Teng, M. Flandes-Iparraguirre, A. Eder, A. Sanchez-Herrero, B. Niranjan, Melbourne Urological Research Alliance (MURAL), Tissue engineered human prostate microtissues reveal key role of mast cell-derived tryptase in potentiating cancer-associated fibroblast (CAF)-induced morphometric transition in vitro, Biomaterials 197 (2019) 72–85, https://doi.org/10.1016/j.biomaterials.2018.12.030.

[21] T. Zadvornyi, N. Lukianova, T. Borikun, A. Tymoshenko, O. Mushii, O. Voronina, I. Vitruk, E. Stakhovskyi, V. Chekhun, Mast cells as a tumor microenvironment factor associated with the aggressiveness of prostate cancer, Neoplasma 69 (2022) 1490–1498, https://doi.org/10.4149/neo_2022_221014N1020.

[22] H.A. Hempel, N.S. Cuka, I. Kulac, J.R. Barber, T.C. Cornish, E.A. Platz, A.M. De Marzo, K.S. Sfanos, Low intratumoral mast cells are associated with a higher risk of prostate cancer recurrence, Prostate 77 (2017) 412–424, https://doi.org/10.1002/pros.23280.

[23] Y. Hu, J. Liu, J. Yu, F. Yang, M. Zhang, Y. Liu, S. Ma, X. Zhou, J. Wang, Y. Han, Identification and validation a costimulatory molecule gene signature to predict the prognosis and immunotherapy response for hepatocellular carcinoma, Cancer Cell Int. 22 (2022) 97, https://doi.org/10.1186/s12935-022-02514-0.

[24] P. Song, W. Li, L. Guo, J. Ying, S. Gao, J. He, Identification and validation of a novel signature based on NK cell marker genes to predict prognosis and immunotherapy response in lung adenocarcinoma by integrated analysis of single-cell and bulk RNA-sequencing, Front. Immunol. 13 (2022) 850745, https://doi.org/10.3389/fimmu.2022.850745.

[25] I. Korsunsky, N. Millard, J. Fan, K. Slowikowski, F. Zhang, K. Wei, Y. Baglaenko, M. Brenner, P. Loh, S. Raychaudhuri, Fast, sensitive and accurate integration of single-cell data with Harmony, Nat. Methods 16 (2019) 1289–1296, https://doi.org/10.1038/s41592-019-0619-0.

[26] N.A. Mabbott, J. Baillie, H. Brown, T.C. Freeman, D.A. Hume, An expression atlas of human primary cells: inference of gene function from coexpression networks, BMC Genom. 14 (2013) 632, https://doi.org/10.1186/1471-2164-14-632.

[27] J. Liu, T. Lichtenberg, K.A. Hoadley, L.M. Poisson, A.J. Kovatich, An integrated TCGA pan-cancer clinical data resource to drive high-quality survival outcome analytics, Cell 173 (2018) 400–416.e11, https://doi.org/10.1016/j.cell.2018.02.052.

[28] P. Geeleher, N.J. Cox, R.S. Huang, Clinical drug response can be predicted using baseline gene expression levels and in vitro drug sensitivity in cell lines, Genome Biol. 15 (2014) R47, https://doi.org/10.1186/gb-2014-15-3-r47.

[29] N.A. Mabbott, J. Baillie, H. Brown, T.C. Freeman, D.A. Hume, An expression atlas of human primary cells: inference of gene function from coexpression networks, BMC Genom. 14 (2013) 632, https://doi.org/10.1186/1471-2164-14-632.

[30] I. Heidegger, G. Fotakis, A. Offermann, J. Goveia, S. Daum, S. Salcher, A. Noureen, H. Timmer-Bosscha, G. Schäfer, A. Walenkamp, S. Perner, A. Beatovic, M. Moisse, C. Plattner, A. Krogsdam, J. Haybaeck, S. Sopper, S. Thaler, M.A. Keller, H. Klocker, Z. Trajanoski, D. Wolf, A. Pircher, Comprehensive characterization of the prostate tumor microenvironment identifies CXCR4/CXCL12 crosstalk as a novel antiangiogenic therapeutic target in prostate cancer, Mol. Cancer 21 (2022) 132, https://doi.org/10.1186/s12943-022-01597-7.

[31] J.A. Brockman, S. Alanee, A.J. Vickers, P.T. Scardino, D.P. Wood, A.S. Kibel, D.W. Lin, F.J. Bianco Jr., D.M. Rabah, E.A. Klein, J.P. Ciezki, T. Gao, M.W. Kattan, A.J. Stephenson, Nomogram predicting prostate cancer–specific mortality for men with biochemical recurrence after radical prostatectomy, Eur. Urol. 67 (2015) 1160–1167, https://doi.org/10.1016/j.eururo.2014.09.019.

[32] U.G. Falagario, A. Abbadi, S. Remmers, L. Björnebo, D. Bogdanovic, A. Martini, A. Valdman, G. Carrieri, M. Menon, O. Akre, M. Eklund, T. Nordström, H. Grönberg, A. Lantz, P. Wiklund, Biochemical recurrence and risk of mortality following radiotherapy or radical prostatectomy, JAMA Netw. Open 6 (2023) e2332900, https://doi.org/10.1001/jamanetworkopen.2023.32900.

[33] D. Ribatti, Mast cells and macrophages exert beneficial and detrimental effects on tumor progression and angiogenesis, Immunol. Lett. 152 (2013) 83–88, https://doi.org/10.1016/j.imlet.2013.05.003.

[34] A.J. Gentles, A.M. Newman, C.L. Liu, S.V. Bratman, W. Feng, D. Kim, V.S. Nair, Y. Xu, A. Khuong, C.D. Hoang, M. Diehn, R.B. West, S.K. Plevritis, A.A. Alizadeh, The prognostic landscape of genes and infiltrating immune cells across human cancers, Nat. Med. 21 (2015) 938–945, https://doi.org/10.1038/nm.3909.

[35] S.I. Shpyleva, V.P. Tryndyak, O. Kovalchuk, A. Starlard-Davenport, V.F. Chekhun, F.A. Beland, I.P. Pogribny, Role of ferritin alterations in human breast cancer cells, Breast Cancer Res. Treat. 126 (2011) 63–71, https://doi.org/10.1007/s10549-010-0849-4.

[36] Y. Luo, C. Liu, Y. Yao, X. Tang, E. Yin, Z. Lu, N. Sun, J. He, A comprehensive pan-cancer analysis of prognostic value and potential clinical implications of FTH1 in cancer immunotherapy, Cancer Immunol. Immunother. 73 (2024) 37, https://doi.org/10.1007/s00262-023-03625-x.

[37] B. Pandya Shesh, V. Walter, K. Palsa, B. Slagle-Webb, E. Neely, T. Schell, J.R. Connor, Sexually dimorphic effect of H-ferritin genetic manipulation on survival and tumor microenvironment in a mouse model of glioblastoma, J. Neuro Oncol. 164 (2023) 569–586, https://doi.org/10.1007/s11060-023-04415-2.

[38] G. Yang, Q. Pan, Y. Lu, J. Zhu, X. Gou, miR-29a-5p modulates ferroptosis by targeting ferritin heavy chain FTH1 in prostate cancer, Biochem. Biophys. Res. Commun. 652 (2023) 6–13, https://doi.org/10.1016/j.bbrc.2023.02.030.

[39] L. Zeng, X. Lyu, J. Yuan, Y. Chen, H. Wen, L. Zhang, J. Shi, B. Liu, W. Li, S. Yang, STMN1 promotes tumor metastasis in non-small cell lung cancer through microtubule-dependent and nonmicrotubule-dependent pathways, Int. J. Biol. Sci. 20 (2024) 1509–1527, https://doi.org/10.7150/ijbs.84738.

[40] Z. Pan, Q. Fang, L. Li, Y. Zhang, T. Xu, Y. Liu, X. Zheng, Z. Tan, P. Huang, M. Ge, HN1 promotes tumor growth and metastasis of anaplastic thyroid carcinoma by interacting with STMN1, Cancer Lett. 501 (2021) 31–42, https://doi.org/10.1016/j.canlet.2020.12.026.

[41] B.V.S.K. Chakravarthi, D.S. Chandrashekar, S. Agarwal, S.A.H. Balasubramanya, S.S. Pathi, M.T. Goswami, X. Jing, R. Wang, R. Mehra, I.A. Asangani, A. M. Chinnaiyan, U. Manne, G. Sonpavde, G.J. Netto, J. Gordetsky, S. Varambally, miR-34a regulates expression of the stathmin-1 oncoprotein and prostate cancer progression, Mol. Cancer Res. 16 (2018) 1125–1137, https://doi.org/10.1158/1541-7786.MCR-17-0230.

[42] E. Zhang, C. Li, Y. Fang, N. Li, Z. Xiao, C. Chen, B. Wei, H. Wang, J. Xie, Y. Miao, Z. Zeng, H. Huang, STMN1 as a novel prognostic biomarker in HCC correlating with immune infiltrates and methylation, World J. Surg. Oncol. 20 (2022) 301, https://doi.org/10.1186/s12957-022-02768-y.

[43] Q. Mao, Z. Chen, K. Wang, R. Xu, H. Lu, X. He, Prognostic role of high stathmin 1 expression in patients with solid tumors: evidence from a meta-analysis, Cell. Physiol. Biochem. 50 (2018) 66–78, https://doi.org/10.1159/000493958.

[44] Y. Cai, L. Bjermer, T.S. Halstensen, Bronchial mast cells are the dominating LTC4S-expressing cells in aspirin-tolerant asthma, Am. J. Respir. Cell Mol. Biol. 29 (2003) 683–693, https://doi.org/10.1165/rcmb.2002-0174OC.

[45] H.E.A. Ali, P.-Y. Lung, A.B. Sholl, S.A. Gad, J.J. Bustamante, H.I. Ali, J.S. Rhim, G. Deep, J. Zhang, Z.Y. Abd Elmageed, Dysregulated gene expression predicts tumor aggressiveness in African-American prostate cancer patients, Sci. Rep. 8 (2018) 16335, https://doi.org/10.1038/s41598-018-34637-8.

[46] J.A. Hamerman, M. Ni, J.R. Killebrew, C. Chu, C.A. Lowell, The expanding roles of ITAM adapters FcRγ and DAP12 in myeloid cells, Immunol. Rev. 232 (2009) 42–58, https://doi.org/10.1111/j.1600-065X.2009.00841.x.

[47] K. Töpfer, M. Cartellieri, S. Michen, R. Wiedemuth, N. Müller, D. Lindemann, M. Bachmann, M. Füssel, G. Schackert, A. Temme, DAP12-based activating chimeric antigen receptor for NK cell tumor immunotherapy, J. Immunol. 194 (2015) 3201–3212, https://doi.org/10.4049/jimmunol.1400330.

[48] M. Belleri, P. Chiodelli, M. Corli, M. Capra, M. Presta, Oncosuppressive and oncogenic activity of the sphingolipid-metabolizing enzyme β-galactosylceramidase, Biochim. Biophys. Acta Rev. Canc 1877 (2022) 188675, https://doi.org/10.1016/j.bbcan.2021.188675.

[49] M. Yang, Z. Jiang, G. Yao, Z. Wang, J. Sun, H. Qin, H. Zhao, GALC triggers tumorigenicity of colorectal cancer via senescent fibroblasts, Front. Oncol. 10 (2020) 380, https://doi.org/10.3389/fonc.2020.00380.

[50] F. He, J. Yu, J. Yang, S. Wang, A. Zhuang, H. Shi, X. Gu, X. Xu, P. Chai, R. Jia, m6A RNA hypermethylation-induced BACE2 boosts intracellular calcium release and accelerates tumorigenesis of ocular melanoma, Mol. Ther. 29 (2021) 2121–2133, https://doi.org/10.1016/j.ymthe.2021.02.014.

[51] J. Moskovitz, S. Bar-Noy, W.M. Williams, J. Requena, B.S. Berlett, E.R. Stadtman, Methionine sulfoxide reductase (MsrA) is a regulator of antioxidant defense and lifespan in mammals, Proc. Natl. Acad. Sci. U. S. A. 98 (2001) 12920–12925, https://doi.org/10.1073/pnas.231472998.

[52] K. Chen, H. Liu, Z. Liu, S. Luo, E.F. Patz, P.G. Moorman, L. Su, S. Shen, D.C. Christiani, Q. Wei, Genetic variants in RUNX3, AMD1 and MSRA in the methionine metabolic pathway and survival in nonsmall cell lung cancer patients, Int. J. Cancer 145 (2019) 621–631, https://doi.org/10.1002/ijc.32128.

[53] Y.-Y. Liu, C. Ge, H. Tian, J.-Y. Jiang, F.-Y. Zhao, H. Li, T.-Y. Chen, M. Yao, J.-J. Li, The transcription factor Ikaros inhibits cell proliferation by downregulating ANXA4 expression in hepatocellular carcinoma, Am. J. Cancer Res. 7 (2017) 1285–1297.

[54] T. Yan, S. Zhu, Y. Shi, C. Xie, M. Zhu, Y. Zhang, C. Wang, C. Guo, Pan-cancer analysis of atrial-fibrillation-related innate immunity gene ANXA4, Front Cardiovasc Med 8 (2021) 713983, https://doi.org/10.3389/fcvm.2021.713983.

[55] J. Liu, H. Wang, M. Zheng, L. Deng, X. Zhang, B. Lin, p53 and ANXA4/NF-κB p50 complexes regulate cell proliferation, apoptosis and tumor progression in ovarian clear cell carcinoma, Int. J. Mol. Med. 46 (2020) 2102–2114, https://doi.org/10.3892/ijmm.2020.4757.

[56] Y. Peng, Z. Zhang, A. Zhang, C. Liu, Y. Sun, Z. Peng, Y. Liu, Membrane-cytoplasm translocation of annexin A4 is involved in the metastasis of colorectal carcinoma, Aging (Albany NY) 13 (2021) 10312–10325, https://doi.org/10.18632/aging.202793.

[57] B. Wei, C. Guo, S. Liu, M.-Z. Sun, Annexin A4 and cancer, Clin. Chim. Acta 447 (2015) 72–78, https://doi.org/10.1016/j.cca.2015.05.016.

[58] P. Li, Y. Wang, L. Zhang, Y. Ning, L. Zan, The expression pattern of PLIN2 in differentiated adipocytes from qinchuan cattle analysis of its protein structure and interaction with CGI-58, Int. J. Mol. Sci. 19 (2018) 1336, https://doi.org/10.3390/ijms19051336.

[59] Q. Cao, H. Ruan, K. Wang, Z. Song, L. Bao, T. Xu, H. Xiao, C. Wang, G. Cheng, J. Tong, X. Meng, D. Liu, H. Yang, K. Chen, X. Zhang, Overexpression of PLIN2 is a prognostic marker and attenuates tumor progression in clear cell renal cell carcinoma, Int. J. Oncol. 53 (2018) 137–147, https://doi.org/10.3892/ijo.2018.4384.

[60] L. Ippolito, G. Comito, M. Parri, M. Iozzo, A. Duatti, F. Virgilio, N. Lorito, M. Bacci, E. Pardella, G. Sandrini, F. Bianchini, R. Damiano, L. Ferrone, G. la Marca, S. Serni, P. Spatafora, C.V. Catapano, A. Morandi, E. Giannoni, P. Chiarugi, Lactate rewires lipid metabolism and sustains a metabolic-epigenetic Axis in prostate cancer, Cancer Res. 82 (2022) 1267–1282, https://doi.org/10.1158/0008-5472.CAN-21-0914.

[61] J.M. Garner, M.J. Herr, K.B. Hodges, L.K. Jennings, The utility of tetraspanin CD9 as a biomarker for metastatic clear cell renal cell carcinoma, Biochem. Biophys. Res. Commun. 471 (2016) 21–25, https://doi.org/10.1016/j.bbrc.2016.02.008.

[62] E.S. Martens-Uzunova, G.D. Kusuma, S. Crucitta, H.K. Lim, C. Cooper, J.E. Riches, A. Azad, T. Ochiya, G.M. Boyle, M.C. Southey, M. Del Re, R. Lim, G.A. Ramm, G.W. Jenster, C. Soekmadji, Androgens alter the heterogeneity of small extracellular vesicles and the small RNA cargo in prostate cancer, J. Extracell. Vesicles 10 (2021) e12136, https://doi.org/10.1002/jev2.12136.

[63] T.A. Wynn, IL-13 effector functions, Annu. Rev. Immunol. 21 (2003) 425–456, https://doi.org/10.1146/annurev.immunol.21.120601.141142.

[64] J.D. Proto, A.C. Doran, G. Gusarova, A. Yurdagul, E. Sozen, M. Subramanian, M.N. Islam, C.C. Rymond, J. Du, J. Hook, G. Kuriakose, J. Bhattacharya, I. Tabas, Regulatory T cells promote macrophage efferocytosis during inflammation resolution, Immunity 49 (2018) 666–677.e6, https://doi.org/10.1016/j.immuni.2018.07.015.

[65] R. Jannoo, Z. Xia, P.E. Row, V. Kanamarlapudi, Targeting of the interleukin-13 receptor (IL-13R)α2 expressing prostate cancer by a novel hybrid lytic peptide, Biomolecules 13 (2023) 356, https://doi.org/10.3390/biom13020356.

[66] K. Wareham, C. Vial, R. Wykes, P. Bradding, E. Seward, Functional evidence for the expression of P2X1, P2X4 and P2X7 receptors in human lung mast cells, Br. J. Pharmacol. 157 (2009) 1215–1224, https://doi.org/10.1111/j.1476-5381.2009.00287.x.

[67] A. Aakula, P. Kohonen, S.-K. Leivonen, R. Mäkelä, P. Hintsanen, J.P. Mpindi, E. Martens-Uzunova, T. Aittokallio, G. Jenster, M. Perälä, O. Kallioniemi, P. Östling, Systematic identification of MicroRNAs that impact on proliferation of prostate cancer cells and display changed expression in tumor tissue, Eur. Urol. 69 (2016) 1120–1128, https://doi.org/10.1016/j.eururo.2015.09.019.
[68] C. Lin, J. He, X. Tong, L. Song, Copper homeostasis-associated gene PRNP regulates ferroptosis and immune infiltration in breast cancer, PLoS One 18 (2023) e0288091, https://doi.org/10.1371/journal.pone.0288091.
[69] D. Le Corre, A. Ghazi, R. Balogoun, C. Pilati, T. Aparicio, S. Martin-Lannerée, L. Marisa, F. Djouadi, V. Poindessous, C. Crozet, J.-F. Emile, C. Mulot, K. Le Malicot, V. Boige, H. Blons, A. de Reynies, J. Taieb, F. Ghiringhelli, J. Bennouna, J.-M. Launay, P. Laurent-Puig, S. Mouillet-Richard, The cellular prion protein controls the mesenchymal-like molecular subtype and predicts disease outcome in colorectal cancer, EBioMedicine 46 (2019) 94–104, https://doi.org/10.1016/j.ebiom.2019.07.036.
[70] M. Choi, S. Moon, H.J. Eom, S.M. Lim, Y.H. Kim, S. Nam, High expression of PRNP predicts poor prognosis in Korean patients with gastric cancer, Cancers 14 (2022) 3173, https://doi.org/10.3390/cancers14133173.
[71] T.G. Phan, P.I. Croucher, The dormant cancer cell life cycle, Nat. Rev. Cancer 20 (2020) 398–411, https://doi.org/10.1038/s41568-020-0263-0.
[72] S.L. Shiao, G.C.-Y. Chu, L.W.K. Chung, Regulation of prostate cancer progression by the tumor microenvironment, Cancer Lett. 380 (2016) 340–348, https://doi.org/10.1016/j.canlet.2015.12.022.
[73] A. Erlandsson, J. Carlsson, M. Lundholm, A. Fält, S.-O. Andersson, O. Andrén, S. Davidsson, M2 macrophages and regulatory T cells in lethal prostate cancer, Prostate 79 (2019) 363–369, https://doi.org/10.1002/pros.23742.
[74] A. Kotsakis, F. Koinis, A. Katsarou, M. Gioulbasani, D. Aggouraki, N. Kentepozidis, V. Georgoulias, E.-K. Vetsika, Prognostic value of circulating regulatory T cell subsets in untreated non-small cell lung cancer patients, Sci. Rep. 6 (2016) 39247, https://doi.org/10.1038/srep39247.
[75] L. Chen, D.B. Flies, Erratum: molecular mechanisms of T cell co-stimulation and co-inhibition, Nat. Rev. Immunol. 13 (2013) 542, https://doi.org/10.1038/nri3484.